

Padé-related resummations of the pressure of quark-gluon plasma by approximate inclusion of g_s^6 -terms

G. Cvetic*

Department of Physics, Universidad Técnica Federico Santa María, Valparaíso, Chile

R. Kögerler†

Department of Physics, Universität Bielefeld, 33501 Bielefeld, Germany

(Dated: October 30, 2018)

We perform various resummations of the hot QCD pressure based on the actual knowledge of the perturbation series which includes the $\sim g_s^6 \ln(1/g_s)$ and part of the $\sim g_s^6$ terms. Resummations are performed separately for the short- and long-distance parts. The $\sim g_s^6$ term of the short-distance pressure is estimated on the basis on the known UV cutoff dependence of the long-distance part. The resummations are of the Padé and Borel-Padé type, using in addition the (Padé-)resummed expression for the squared Debye screening mass m_E^2 and, in some cases, even for the EQCD coupling parameter g_E^2 . The resummed results depend weakly on the yet unknown $\sim g_s^6$ terms and on the the short-range renormalization scale, at all temperatures. The dependence on the long-range renormalization scale is appreciable at low temperatures $T \lesssim 1$ GeV. The resulting dependence of pressure on temperature T is compatible with the results of the lattice calculations at low T .

PACS numbers: 12.38.Cy, 11.10.Wx, 12.38.Bx, 12.38.Mh

I. INTRODUCTION AND DESCRIPTION OF THE APPROACH

Today we have at our disposal a well-elaborated technique for perturbatively treating field theory at finite temperature and/or chemical potential [1]. This formalism goes far beyond the ordinary ($T = 0$) perturbation theory insofar as a correct treatment of infrared divergences (specifically those which are connected with $T \neq 0$) requires partial resummation of infinitely many specific diagrams. This implies – among other things – that the infrared convergent perturbative expressions come out as series in g_s (the fundamental coupling constant) rather than in g_s^2 [or $a = g_s^2/(4\pi^2)$].

During the last decade, several physical quantities, the most prominent example being the free energy density F of the quark-gluon plasma, have been calculated within this formalism up to $\mathcal{O}(g_s^5)$ [2, 3] and (partially) even to $\mathcal{O}(g_s^6)$ [4, 5]. Disappointingly, in spite of the relatively high orders available, the results are of very limited applicability even at very high temperatures ($T \gtrsim 1$ TeV) where g_s certainly becomes small. In fact, if successive terms in the perturbative series are added, the corresponding truncated sum changes dramatically, jumping up and down. Furthermore, the unphysical dependence on the renormalization scale is strong and seems to become even stronger with increasing order (the renormalization scale in $\overline{\text{MS}}$ scheme will be denoted as $\overline{\mu}$, and in a general scheme as μ). Both effects considerably reduce the reliability of the perturbative results for representing physical quantities and have therefore been object of intensive theoretical studies.

Ways out of the convergence dilemma are in general looked for by either performing some clever resummations or by reorganizing perturbation theory in some way (actually, in some cases, this amounts to the same thing) [1]. Several specific approaches have been applied up to now. Among them are quasi-particle models [6], Φ -derivable approximations [7], screened [8] or optimized [9] perturbation theory, hard thermal loop perturbation theory [10].

Within the present paper we concentrate mainly on the question of renormalization scale (RS $\overline{\mu}$) dependence of the resummed results, in $\overline{\text{MS}}$ scheme, as well as on the dependence of the results on the yet unknown part of the g_s^6 -term in truncated perturbation series. The resummation approaches mentioned above do have some residual renormalization scale dependence. Furthermore, the conventional choice for the RS $\overline{\mu}$ at finite T ($\overline{\mu} \simeq 2\pi T$) is not natural since different energy scales get involved in all calculations (see later).

In order to improve this situation, we replace the (partially resummed) perturbation series by approximants which are more stable under the variation of $\overline{\mu}$. The Padé approximants (PA's) [11, 12, 13, 14] and other Padé-related resummations, such as Borel-Padé (BPA's) [15] and modified Baker-Gammel approximants (mBGA's) [16, 17], are

*Electronic address: gorazd.cvetic@usm.cl

†Electronic address: koeg@physik.uni-bielefeld.de

known in general to reduce the unphysical $\bar{\mu}$ -dependence significantly (mBGA's even entirely). Usually these approximants are applied to a given truncated perturbation series (TPS) of a given order, and they fulfill in addition the "minimal" requirement: upon re-expanding them in powers of the coupling parameter, they reproduce the TPS to the given order. In this sense they are sometimes considered to be some sort of mathematical artifice without any deeper physical motivation. This opinion is delusive, however, because of several reasons:

1. The basis of all field theoretic approaches is the path integral expression for the generating functional which has to be attributed a specific mathematical meaning. In ordinary perturbation theory this is achieved by Taylor expanding the corresponding exponential of the interaction Lagrangian leading to the well-known power series. But this is by no means better or more natural than by approximating it in terms of other approximants (e.g., Padé) – we are only less used to it. In some sense Padé or Padé-related sequences seem even more adapted than power series since they allow for (pole) singularities, and we know that most physical amplitudes do include singularities.
2. The asymptotically divergent nature of the expansion in powers of the coupling parameters represents a practical problem concerning the actual evaluation, and calls for, among other things, nonperturbative information in order to fix the renormalon ambiguities and to produce unique predictions. On the other hand, due to the generally better convergence of Padé and Padé-related approximants, one hopes that the convergence of the corresponding sequence of the (Padé-)resummed TPS's will improve and that it would converge to a specific prediction. The Padé sequence, in fact, with increasing order shows convergence under rather general conditions even when the corresponding TPS is (asymptotically) divergent [11].
3. It can be shown that PA's (and mBGA's) can be represented by weighted averages of running coupling parameter (one-loop running in the case of PA, exact running in the case of mBGA) at specific values of reference momenta [13, 18], and are thus a realization of the fact that each physical quantity in field theory is characterized by specific values of the momentum flow. In this sense they represent different approximations to the Neubert's formalism [19] of renormalization improved perturbation theory.

From the diagrammatic point of view, PA and Padé-related methods represent a resummation of those (infinitely many) diagrams which – when added – approximately (or exactly) cancel the $\bar{\mu}$ -dependence of the given quantity.

PA's, BPA's and mBGA's have been applied to TPS for several QCD or QED quantities at zero temperature (see, for example, Refs. [14, 15, 17]) and have often led to significant improvement of the RS-dependence problem. Recently, same types of approximation have also been used for similar purposes in finite temperature gauge theory: PA's in Refs. [20, 21]; somewhat related Borel methods in Refs. [22], by discerning some information on renormalons (for renormalon properties in ϕ^4 theory at finite T , see Ref. [23]). The first PA resummations at finite- T [20] consisted in simply replacing the available power series (in powers of g_s) for the entire QCD free energy by various PA's. Although the results demonstrate a weakened $\bar{\mu}$ -dependence, we regard some aspects of this approach as problematic. Our reservation is due to the simple observation that two ingredients – (a) the infrared stable TPS of thermal field theory, and (b) the Padé(-related) approximations applied to this TPS – imply resummation of infinitely many terms. The corresponding classes of diagrams are, however, neither equivalent nor disjunct. Therefore, care has to be taken to avoid double counting and to disentangle the various resummations.

Recently, we have developed a formalism to consistently treat this problem [21]. The procedure is the following: Consider some physical quantity and its TPS (to a given order) in thermal field theory. We specifically have in mind the static pressure p_{QCD} of the QCD plasma, i.e., the negative of the free energy density F_{QCD} . It is connected to the partition function \mathcal{Z} by the relation

$$p_{\text{QCD}} = -F_{\text{QCD}} = \lim_{V \rightarrow \infty} \frac{T}{V} \ln \mathcal{Z} , \quad (1)$$

$$\mathcal{Z} = \int \mathcal{D}A_\mu^a \mathcal{D}\psi \mathcal{D}\bar{\psi} \exp \left(- \int_0^{1/T} d\tau \int d^3x \mathcal{L}_{\text{QCD}} \right) , \quad (2)$$

where \mathcal{L}_{QCD} is the (Euclidean) QCD-Lagrangian density, T is the temperature, V is the three-dimensional volume, and the renormalization convention $p_{\text{QCD}}(T=0) = 0$ is taken; g_s is the QCD gauge coupling parameter. The corresponding TPS has the generic structure

$$p = p_{\text{ideal}} [C_0 + C_2 g_s^2 + C_3 g_s^3 + C_4 g_s^4 + C_5 g_s^5 + C_6 g_s^6 + \dots] , \quad (3)$$

where the coefficients C_i may include contributions of order $\ln g_s$. The terms proportional to odd powers of g_s [or, equivalently, fractional powers of $a \equiv g_s^2/(4\pi^2)$] are exclusively due to resummation of specific (ring, or daisy)

diagrams, but the latter also contribute to terms proportional to even powers of g_s . Clearly g_s and the coefficients C_i depend on the chosen renormalization scheme and, in particular, on the renormalization scale $\bar{\mu}$ ($\propto T$). Due to the asymptotic freedom we expect that g_s becomes sufficiently small at large temperature T . In the following, we concentrate on such a large- T situation.

The first step needed for the application of the formalism of Ref. [21] is the separation in Eq. (3) of the purely perturbative part from the contributions stemming from the (ring-)resummations. This can be done in an unambiguous and consistent way, since the resummation terms represent exclusively the contributions of the (bosonic) zero modes to the considered physical quantity. Note in this respect that resummation is needed purely for taming the finite- T infrared divergences, and only the infrared parts of the higher order diagrams contribute to the (finite) order terms. Therefore, the identification of the contributions from the zero modes (long-range contributions) is needed. This can be achieved either by integrating out directly the high momentum regime or, more elegantly, by utilizing the effective field formalism [3, 27] based on dimensional reduction method Refs. [3, 27, 28, 29]. The idea behind is that (at high enough temperature, with g_s sufficiently small) the four-dimensional thermal QCD at length scales $\gtrsim 1/(g_s T)$ is equivalent to an effective three-dimensional field theory of (static) boson fields. This effective theory represents the physics of the zero bosonic modes and thus reproduces all static correlations of the original QCD at the aforementioned distances. Consequently, the contribution of the zero modes to the partition functions or to the pressure can be calculated by means of the effective theory. Within QCD the long-distance part can be further subdivided corresponding to the two regimes $R \sim 1/(g_s T)$ (determined by color-electric screening) and $R \simeq 1/(g_s^2 T)$ (color-magnetic screening). Denoting the corresponding contributions to p (or F) by the subscripts M and G, respectively, the final decomposition corresponding to the three energy regions is

$$p = p_E + p_M + p_G . \quad (4)$$

Here, p_E denotes the short-distance, and $p_M + p_G \equiv p_{M+G}$ the zero-mode long-distance contribution.

Now comes one of the main points of the formalism of Ref. [21]: Having the separation (4) of the pressure into p_E and p_{M+G} , we can argue that both are separately physical quantities, and thus both, when calculated to all orders, are separately $\bar{\mu}$ -independent. The reason for it is shown by the following indirect argument: Consider any (static) two-point-correlator within the given field theory. It is a measurable quantity and so is its long-range behaviour. But the latter is determined solely by the exchange of zero modes (note that the exchange of a mode with frequency ω_n contributes a term to the correlator which vanishes like $\exp(-|\omega_n|R)$ at $R \rightarrow \infty$, thus the only surviving contribution at large distances is the one with $\omega_0 = 0$). Thus the contribution of ω_0 to each correlator is measurable (and therefore $\bar{\mu}$ -independent) once we have fixed, by convention, the minimal value R_{\min} of what we consider large distances (or: factorization scale $\Lambda_E \sim 1/R_{\min}$). Since these correlators are derived from the partition function \mathcal{Z} by means of functional derivatives, even the zero-mode contribution to \mathcal{Z} , and thus also to p , is $\bar{\mu}$ -independent (physical). Consequently, the remaining part of the measurable pressure – the short-range contribution p_E represented by the ordinary perturbative terms – must also be $\bar{\mu}$ -independent. The RS-independence of both parts separately has been demonstrated analytically in Ref. [21] by using the known perturbation series (up to order g^5).

The separation and the $\bar{\mu}$ -independence of the separate terms allows a more consistent application of Padé and Padé-related approximations: they are applied to TPS's of each quantity p_E and p_{M+G} separately.¹ We can illustrate the importance of using separate approximations with a simple example – the Padé-resummation of a quantity $S \equiv (S_1 + S_2)$, where S_1 and S_2 are separately physical quantities, each of them available as power series of a up to next-to-leading order (NLO):

$$S_j = a(1 + r_{(j)}a) + \mathcal{O}(a^3) \quad (j=1,2) . \quad (5)$$

When we apply to the TPS of the sum S a PA, say $[1/1](a)$, and then expand this back in powers of the coupling a , we obtain

$$S^{[1/1]} = 2a \left[1 - \frac{1}{2}(r_{(1)} + r_{(2)})a \right]^{-1} = 2a \left[1 + \frac{1}{2}(r_{(1)} + r_{(2)})a + \frac{1}{4}(r_{(1)}^2 + r_{(2)}^2 + 2r_{(1)}r_{(2)})a^2 \right] + \mathcal{O}(a^4) . \quad (6)$$

The coefficient at $\sim a^3$ here has a term $2r_{(1)}r_{(2)}$. Therefore, the Padé-resummed S contains mixing effects at $\sim a^3$, i.e., an interference effect between the two amplitudes for the physical observables S_1 and S_2 . This is not acceptable, because S is the (incoherent) sum of S_1 and S_2 . Therefore, the PA should not be applied to the entire sum S , but

¹ Since only little information is available about p_G , we will find it more convenient to apply Padé(-related) resummations to p_{M+G} and not separately to p_M and p_G .

separately to S_1 and S_2 . This argument holds also when different PA's or Padé-related resummations are applied, and when the order of the TPS is higher.

One of the consequences of the separate treatment of p_E and p_{M+G} is that the natural renormalization scale $\bar{\mu}$ used in these two quantities should be of the order of the energy of the modes contributing to them: $\bar{\mu} \sim 2\pi T$ in p_E , and $\bar{\mu} \lesssim g_s T$ in p_{M+G} .

Within the present paper we will apply Padé (PA) and Borel-Padé approximants (BPA's) to the evaluation of p_{QCD} . The modified Baker-Gammel approximants (mBGA's), which are $\bar{\mu}$ -independent [16] or even renormalization scheme independent [17], are technically more involved. An analysis with mBGA's, which at least could serve as some kind of quality control of the general procedure, will be presented elsewhere. On the other hand, BPA's are also applied here and they represent an extension of the Padé analysis: PA's are applied to the corresponding TPS's of the Borel transforms, and then the resummed quantity is obtained by Borel integration. This procedure gets its motivation from the hope that the Borel summation might defuse the notorious divergence problem of perturbation theory, as well as from the fact that the power expansion of the Borel transform has significantly better convergence properties than the original series and is thus more amenable to the Padé-type resummations.

One technical remark should be added here – the separation of the energy range into a high and a low energy region requires introduction of a factorization scale Λ_E which defines a boundary between the two: $2\pi T > \Lambda_E > g_s T$. Consequently, the two contributions separated in the described way acquire an artificial dependence on Λ_E , although the sum of the two terms $p_E + p_{M+G}$ has to be Λ_E -independent. Similarly, for the individual terms p_E and p_{M+G} to have physical meaning themselves, the factorization scale should be suitably chosen. Technically this means that the approximants for p_E and p_{M+G} , although independent of each other, should be chosen such that the Λ_E -dependence is minimized.

In our previous paper [21] we applied this procedure to calculation of the free energy (pressure) both in QCD with n_f (massless) quarks and in a ϕ^4 -theory. At that time the relevant TPS's had been calculated only up to terms of order g_s^5 with the following implications for the perturbative structure of the relevant contributions: The short-distance term $F_E (= p_E)$ is determined perturbatively up to NLO [in $a \equiv a(\bar{\mu}) \equiv g_s^2(\bar{\mu})/(2\pi)^2$]

$$F_E/F_{\text{ideal}} = p_E/p_{\text{ideal}} = 1 - B(n_f)\tilde{F}_E, \quad (7)$$

$$\tilde{F}_E = a \{1 + C_E(n_f, \Lambda_E, \bar{\mu})a\}, \quad (8)$$

and so is the electric (Debye) screening mass m_E

$$\tilde{m}_E^2 \equiv \frac{1}{4\pi^2 T^2} \frac{1}{(1 + n_f/6)} m_E^2 = a \{1 + C_M(n_f, \bar{\mu})a\} \quad (9)$$

The long-distance part was a power series in g_s [$\equiv g_s(\bar{\mu})$] up to order g_s^2

$$F_M = -p_M = -\frac{2}{3\pi} T m_E^3 \tilde{p}_M, \quad (10)$$

$$\tilde{p}_M = 1 + C_{M1}(n_f, \Lambda_E, \bar{\mu})g_s + C_{M2}(n_f)g_s^2. \quad (11)$$

We refer to Ref. [21] for compilation of explicit expressions for B , C_E , C_M , C_{M1} , C_{M2} . These are rather short power series and they allow construction of only low order Padé approximants, e.g., PA [1/1](a) for F_E and m_E^2 , and PA [0/2](g_s) for \tilde{p}_M . In addition, the TPS for $\tilde{p}_M (= -\tilde{F}_M)$ is very strongly divergent, and the TPS's for \tilde{F}_E and for \tilde{m}_E^2 are divergent to a somewhat lesser extent. Therefore, resummation results based on these TPS's should be taken with care. Nevertheless, the application of these low order approximants yielded results which were fairly stable under the variation of $\bar{\mu}$, although – at low temperatures $T \lesssim 10$ GeV – they deviated substantially from the lattice results [24, 25, 26].

In such a situation, an additional order in the perturbation series (i.e., terms of order g_s^6) is much more than an additional tiny correction, but constitutes a significant enlargement of the basis for Padé approximations, since it adds additionally both to F_E and F_M and (for the first time non-vanishingly) to F_G . Therefore, the calculation of the $\sim g_s^6 \ln(1/g_s)$ contribution to the long-range part of the pressure published in Ref. [4] is extremely gratifying. The full $O(g_s^6)$ contribution cannot be achieved perturbatively because of the well-known breakdown of perturbation theory due to incurable infrared divergences occurring at this order [30, 31]. What can be evaluated is the coefficient of the logarithmic ultraviolet divergence contained in F_G , because of the superrenormalizability of the corresponding effective three-dimensional field theory; and this is exactly the coefficient of the $O(g_s^6 \ln(1/g_s))$ -term in F_G . The term purely proportional to g_s^6 remains unspecified and has to be treated as a free parameter unless information from nonperturbative methods (e.g., lattice calculations) is inferred.

Within the present paper we will utilize the new results [4] on the perturbation expansion of the QCD-pressure as much as possible in order to find approximants which are reasonably stable under RS-variation. This gives us

the freedom of using higher order Padé or Borel-Padé approximants and thus treating the long-range part p_{M+G} ($= -F_{M+G}$) in a more reliable way. Unfortunately, the full four-loop contribution to the short-range part p_E ($= -F_E$), which is in principle perfectly calculable within ordinary perturbation theory and would yield $\mathcal{O}(a^3)$ correction to Eq. (8), is not yet available at the moment. Therefore, we have no direct basis for improving the approximants to p_E . Nevertheless, we can obtain some restricted information about the $\mathcal{O}(g_s^6)$ -terms in p_E from the requirement that p_E be $\bar{\mu}$ -independent and $(p_E + p_{M+G})$ be Λ_E -independent. A constant ($\bar{\mu}$ - and Λ_E -independent) term in the coefficient at $\mathcal{O}(g_s^6)$ in p_E still remains unspecified, but its value can roughly be estimated. The new results of Ref. [4] also allow a better approximation to the parameter g_E^2 of the effective theory, which further improves the resulting predictions.

In Sec. II we describe the separation of the QCD-pressure into contributions stemming from different energy regions and specify the known corresponding effective Lagrangians. We then present the available perturbation expansion of the long- and the short-range contributions and work out the effects of the factorization scales Λ_E and Λ_M (which have not been explicitly disentangled in Ref. [4] because of their simplified treatment of the RS-dependence). In Sec. III, the short-distance and the long-distance parts of the pressure are resummed separately by Padé and/or Borel-Padé approximants, and the selection of approximants is narrowed down by requiring weak residual $\bar{\mu}$ -dependence of p_E and of p_{M+G} , and weak Λ_E -dependence of $(p_E + p_{M+G})$. In Sec. IV the resummed results as a function of temperature T are presented, as well as arguments for narrowing down further the selection of acceptable approximants. In Sec. V, results of TPS evaluations as a function of T are presented, for comparison. In Sec. VI, our results are compared with the predictions obtained within other approaches, in particular with lattice results (which are available only for rather low temperatures), and finish with some concluding remarks. A short compilation of the Padé and Borel-Padé approximants is given in the Appendix.

II. PERTURBATION EXPANSION OF LONG- AND SHORT-DISTANCE PRESSURE

The basic information about the physics of a quark-gluon system in thermal equilibrium at temperature T is contained in the expression for the pressure $p_{\text{QCD}}(T)$ or, equivalently, the free energy density $F_{\text{QCD}}(T)$. In $d + 1$ dimensions ($d = 3 - 2\epsilon$) this is given by Eqs. (1)-(2), with d^3x replaced by $d^d x$. Boundary conditions over the finite time τ direction are periodic for bosons and anti-periodic for fermions.

When the temperature T is above the masses m_q of active quarks, and the QCD gauge coupling g_s is small enough, there are three physically different scales involved: $\sim 2\pi T$, $\sim g_s T$, $\sim g_s^2 T$. The last two correspond to the color-electric and color-magnetic screening, respectively. The decomposition (4) $p_{\text{QCD}} = p_E + p_M + p_G$ reflects the contributions from the aforementioned three energy regimes: p_E are contributions from the modes with energies in the interval $[\Lambda_E, \infty]$, p_M from those in $[\Lambda_M, \Lambda_E]$, p_G from those in $[0, \Lambda_M]$, where the factorization scales Λ_E and Λ_M define the borders between the three energy regimes

$$g_s^2 T < \Lambda_M < g_s T < \Lambda_E < 2\pi T. \quad (12)$$

The long-distance part $p_M + p_G \equiv p_{M+G}$ is due to the bosonic zero (Matsubara) frequency mode, whereas p_E contains all higher modes. For calculating the different parts analytically one most conveniently uses the method of effective Lagrangians [3, 27, 32] based on the dimensional reduction method [3, 27, 28, 29]: Whereas the high-energy regime behavior, which is responsible for p_E , is determined by the original $(d + 1)$ -dimensional QCD Lagrangian, the low-energy regime behavior, responsible for p_{M+G} , can be represented by a d -dimensional effective bosonic theory called electrostatic QCD (EQCD), such that

$$p_{\text{QCD}} = p_E + \frac{T}{V} \ln \int \mathcal{D}A_i^a \mathcal{D}A_0^a \exp \left(- \int d^d x \mathcal{L}_{\text{EQCD}} \right), \quad (13)$$

$$\mathcal{L}_{\text{EQCD}} = \frac{1}{2} \text{Tr} F_{ij}^2 + \text{Tr} [D_i, A_0]^2 + m_E^2 \text{Tr} A_0^2 + \lambda_E^{(1)} (\text{Tr} A_0^2)^2 + \lambda_E^{(2)} \text{Tr} A_0^4 + \dots, \quad (14)$$

where $i = 1, \dots, d$; $F_{ij} = (i/g_E)[D_i, D_j]$, $D_i = \partial_i - ig_E A_i$. The notation $A_\mu = A_\mu^a \bar{T}^a$ is used, with \bar{T}^a being the Hermitean generators of SU(3) normalized to $\text{Tr} \bar{T}^a \bar{T}^b = (1/2)\delta^{ab}$.

The four parameters of the effective theory are the Debye screening mass m_E ($\sim g_s T$), the coupling parameters g_E^2 ($\sim g_s^2 T$) and $\lambda^{(1)}, \lambda^{(2)}$ ($\sim g_s^4 T$) (the latter two are not independent if $d = 3$). These and the hard scale pressure p_E ($\sim T^4$) are obtained by the well-known matching procedure: the parameters as functions of g_s, T (and the UV-cutoff Λ_E of $\mathcal{L}_{\text{EQCD}}$) must be tuned in such a way that the effective theory reproduces the physical effects of the full theory at large distances. The dots in Eq. (14) stand for higher dimensional effective interaction terms which yield corrections $\delta p \sim g_s^7 T^4$ and are thus neglected here.

Due to the separate screening of the color-electric ($m_E \sim g_s T$) and the color-magnetic ($m_M \sim g_s^2 T$) degrees of freedom within QCD, the above EQCD-action can be further decomposed into two parts corresponding to two

physically different energy scales. The color-electric scales ($\sim g_s T$) are separated by integrating out A_0

$$\frac{T}{V} \ln \int \mathcal{D}A_i^a \mathcal{D}A_0^a \exp \left(- \int d^d x \mathcal{L}_{\text{EQCD}} \right) = p_{\text{M}}(T) + \frac{T}{V} \ln \int \mathcal{D}A_i^a \exp \left(- \int d^d x \mathcal{L}_{\text{MQCD}} \right) \quad (15)$$

$$\equiv p_{\text{M}}(T) + p_{\text{G}}(T) , \quad (16)$$

where

$$\mathcal{L}_{\text{MQCD}} = \frac{1}{2} \text{Tr} F_{ij}^2 + \dots \quad (17)$$

represents the Lagrangian density for magnetostatic QCD – the effective theory for the energy region below Λ_{M} , typically energies $\sim g_s^2 T$. Here $F_{ij} = (i/g_{\text{M}})[D_i, D_j]$ with $D_i = \partial_i - ig_{\text{M}} A_i$.

There are two matching coefficients now: the long-distance [$\sim 1/(g_s T)$] pressure p_{M} ($\sim m_{\text{E}}^3 T \sim g_s^3 T^4$) and the coupling parameter g_{M}^2 which is close to g_{E}^2 [33]

$$g_{\text{M}}^2 = g_{\text{E}}^2 (1 + \mathcal{O}(g_{\text{E}}^2/m_{\text{E}})) = g_{\text{E}}^2 (1 + \mathcal{O}(g_s)) . \quad (18)$$

Now we will present the perturbation expansions for p_{X} ($\text{X} = \text{E}, \text{M}, \text{G}$) on the basis of the results of Ref. [4]. The authors of Ref. [4] present each $p_{\text{X}}/(T\tilde{\mu}^{-2\epsilon})$ as² an expansion in powers of the coupling parameters of the respective effective theory. We note that they used dimensional regularization in the $\overline{\text{MS}}$ scheme, thereby invoking a common renormalization scale $\bar{\mu}$ for all p_{X} and for other matching coefficients. Therefore, their results do not contain explicitly the (physical) factorization scales Λ_{E} and Λ_{M} , and contain the unphysical infinite terms $\propto 1/\epsilon$ which cancel in the sum $p_{\text{QCD}} = p_{\text{E}+\text{M}+\text{G}}$. We will obtain our basic formulae on the basis of their aforementioned expansions by replacing in the logarithms of expansion coefficients their renormalization scale $\bar{\mu}$ by the IR and/or UV cutoffs of the respective effective theory,³ and by removing all the terms proportional to $1/\epsilon$ in each $p_{\text{X}}/(T\tilde{\mu}^{-2\epsilon})$ and then taking $\epsilon = 0$ in each p_{X} . While the aforementioned $1/\epsilon$ terms cancel in the sum $p_{\text{E}+\text{M}+\text{G}}/(T\tilde{\mu}^{-2\epsilon})$, the effect of the common factor $1/\tilde{\mu}^{-2\epsilon}$ also disappears (i.e., reduces to one) in this sum when $\epsilon \rightarrow 0$. Which of the $\ln \bar{\mu}$ -terms in the coefficients get replaced by logarithms of the UV scale and which by those of the IR scale of the effective theory – this is unambiguously determined by the requirement that the entire $p_{\text{E}+\text{M}+\text{G}}$ be independent of the factorization scales. On the other hand, the aforementioned procedure to eliminate first the $1/\epsilon$ infinities from each $p_{\text{X}}/(T\tilde{\mu}^{-2\epsilon})$ and then replace $\epsilon \mapsto 0$ to obtain p_{X}/T is certainly not unique. Other procedures would result in expansions for p_{X} which differ from ours by certain constant numbers (independent of scales) in some of the coefficients of the expansion in powers of the coupling parameters of the respective effective theory, this ambiguity being a manifestation of renormalization freedom. The overall sum $p_{\text{E}+\text{M}+\text{G}}$ would remain the same. We note that our procedure leads to the decomposition of Ref. [3], at least to the order available in that Reference. Further, we checked that the re-expansion in powers of QCD coupling parameter $g_s(\bar{\mu})$ of each obtained p_{X} reproduces for the sum $p_{\text{E}+\text{M}+\text{G}}$ the same expansion as the one obtained in Ref. [4].

The expansion of p_{G} starts at $\sim g_{\text{M}}^6$ ($\sim g_s^6$)

$$p_{\text{G}} = T g_{\text{M}}^6 \frac{8 \cdot 3^3}{(4\pi)^4} \left[8 \alpha_{\text{G}} \ln \left(\frac{\Lambda_{\text{M}}}{2m_{\text{M}}} \right) + \delta_{\text{G}} \right] \quad (19)$$

$$\alpha_{\text{G}} = \frac{43}{96} - \frac{157}{6144} \pi^2 \approx 0.195715 , \quad (20)$$

where the value (20) was obtained in [4] and $m_{\text{M}} \equiv 3g_{\text{M}}^2$ ($\sim g_s^2 T$). The coefficient δ_{G} denotes a dimensionless number which is not perturbatively calculable but is expected to be $|\delta_{\text{G}}| \sim 1$ (note that $8\alpha_{\text{G}} \approx 1.6$). We will allow the following, rather generous, variation of δ_{G} :

$$-5 < \delta_{\text{G}} < +5 . \quad (21)$$

We note that, according to the procedure mentioned before, the result (19) is obtained from the corresponding result for $p_{\text{G}}(T)/(T\tilde{\mu}^{-2\epsilon})$ of Ref. [4] by removing the term $1/\epsilon$, replacing in the logarithm $\bar{\mu}$ by the UV cutoff Λ_{M} of MQCD, and then taking $\epsilon \rightarrow 0$.

² $\tilde{\mu} = \bar{\mu}(e^{\gamma_{\text{E}}}/4\pi)^{1/2}$, where $\bar{\mu}$ is the renormalization scale in the $\overline{\text{MS}}$ scheme.

³ For p_{G} (MQCD), the UV cutoff is Λ_{M} ; for p_{M} (EQCD), the IR cutoff is Λ_{M} , and the UV cutoff is Λ_{E} . For p_{E} (QCD), the IR cutoff is Λ_{E} , and the UV cutoff will be taken to be $\bar{\mu}_{\text{E}}$ ($\sim 2\pi T$), i.e., the ($\overline{\text{MS}}$) renormalization scale for $g_s(\bar{\mu}_{\text{E}})$ appearing in p_{E} .

The same procedure gives for p_M the following expression:

$$\begin{aligned}
p_M(T) = & T m_E^3 \left(\frac{2}{3\pi} \right) \left\{ 1 + \frac{1}{4\pi} 3^2 \left(\frac{g_E^2}{m_E} \right) \left[-\frac{3}{4} - \ln \left(\frac{\Lambda_E}{2m_E} \right) \right] \right. \\
& + \frac{1}{(4\pi)^2} 3^3 \left(\frac{g_E^2}{m_E} \right)^2 \left[-\frac{89}{24} - \frac{\pi^2}{6} + \frac{11}{6} \ln 2 \right] \\
& + \frac{1}{(4\pi)^3} 3^4 \left(\frac{g_E^2}{m_E} \right)^3 \left[8(\alpha_M + \alpha_G) \ln \left(\frac{\Lambda_E}{2m_E} \right) - 8 \alpha_G \ln \left(\frac{\Lambda_M}{2m_E} \right) + \beta_M \right] \\
& \left. + \frac{3}{4\pi} \frac{(-5)}{2} \frac{\lambda_E^{(1)}}{m_E} + \dots \right\}, \tag{22}
\end{aligned}$$

The expression in the brackets containing α_M and α_G is obtained from the term $8 \alpha_M \ln(\bar{\mu}/(2m_E))$ in the expansion for $p_M/(T\bar{\mu}^{-2\epsilon})$ of Ref. [4], by replacing $\bar{\mu}$ in part of the logarithm by the corresponding UV cutoff Λ_E of EQCD and in the rest of the logarithm by the IR cutoff Λ_M in such a way as to guarantee that the sum $p_G + p_M$ is independent of Λ_M . For this, relation (18) for g_M must be inserted into expression (19)

$$p_G = T m_E^3 \left(\frac{2}{3\pi} \right) \left(\frac{3^4}{(4\pi)^3} \right) \left(\frac{g_E^2}{m_E} \right)^3 \left[8 \alpha_G \ln \left(\frac{\Lambda_M}{6g_E^2} \right) + \delta_G \right]. \tag{23}$$

In expression (22) for p_M , the values of constants α_M and β_M have been obtained in Refs. [4] and [5], respectively

$$\alpha_M = \frac{43}{32} - \frac{491}{6144} \pi^2 \approx 0.555017, \tag{24}$$

$$\beta_M \approx -1.391512. \tag{25}$$

The last term in expansion (22) is written in the convention $\lambda_E^{(2)} = 0$ were $\lambda_E^{(1)}$ is equal to [34]

$$\lambda_E^{(1)} = T g_s^4(\bar{\mu}) \frac{1}{24\pi^2} (9 - n_f) + \mathcal{O}(g_s^6). \tag{26}$$

Here, n_f is the number of active quark flavors. In ref. [35] a different convention is adopted yielding $\lambda_E^{(1)} = T g_s^4 n_f / (432\pi^2) + \mathcal{O}(g_s^6)$ and $\lambda_E^{(2)} = T g_s^4 (1 - n_f/3) / (24\pi^2) + \mathcal{O}(g_s^6)$, but this then leads to the same result for p_M .

Adding expressions (22) and (23), we obtain the sum p_{M+G} as expansion in powers of the EQCD parameters g_E and m_E

$$\begin{aligned}
\tilde{p}_{M+G} &\equiv \frac{3\pi}{2} \frac{1}{T m_E^3} (p_M + p_G) \\
&= \left\{ 1 + \frac{1}{4\pi} 3^2 \left(\frac{g_E^2}{m_E} \right) \left[-\frac{3}{4} - \ln \left(\frac{\Lambda_E}{2m_E} \right) \right] \right. \\
&\quad + \frac{1}{(4\pi)^2} 3^3 \left(\frac{g_E^2}{m_E} \right)^2 \left[-\frac{89}{24} - \frac{\pi^2}{6} + \frac{11}{6} \ln 2 \right] \\
&\quad \left. + \frac{1}{(4\pi)^3} 3^4 \left(\frac{g_E^2}{m_E} \right)^3 \left[8\alpha_M \ln \left(\frac{\Lambda_E}{2m_E} \right) + 8 \alpha_G \ln \left(\frac{\Lambda_E}{6g_E^2} \right) + \beta_M + \delta_G \right] + \frac{3}{4\pi} \frac{(-5)}{2} \frac{\lambda_E^{(1)}}{m_E} + \dots \right\}. \tag{27}
\end{aligned}$$

The other matching coefficients m_E and g_E can be expanded in powers of QCD coupling $g_s \equiv g_s(\bar{\mu})$ (cf. [4], with $\epsilon \mapsto 0$)

$$m_E^2 = T^2 (1 + n_f/6) g_s^2 \left\{ 1 + \left(\frac{g_s}{2\pi} \right)^2 \left[P_m(n_f) + 2\beta_0 \ln \left(\frac{\bar{\mu}}{2\pi T} \right) \right] + \mathcal{O}(g_s^4) \right\}, \tag{28}$$

$$g_E^2 = T g_s^2 \left\{ 1 + \left(\frac{g_s}{2\pi} \right)^2 \left[P_g(n_f) + 2\beta_0 \ln \left(\frac{\bar{\mu}}{2\pi T} \right) \right] + \mathcal{O}(g_s^4) \right\}, \tag{29}$$

where $\beta_0 = (11/4)(1 - 2n_f/33)$ is the first beta coefficient, and

$$P_m(n_f) = \frac{(0.612377 - 0.488058 n_f - 0.0427979 n_f^2)}{(1 + n_f/6)}, \tag{30}$$

$$P_g(n_f) = (-0.387623 - 0.423454 n_f). \tag{31}$$

The $\lambda_E^{(1)}/m_E$ -term in expansion (27) can be written with the help of the leading order relation (26) and relations (28)-(29) in several ways, for example in the following two ways:

$$\frac{3}{4\pi} \frac{(-5)}{2} \frac{\lambda_E^{(1)}}{m_E} = -\frac{5}{(4\pi)^3} \frac{(9-n_f)}{(1+n_f/6)^{1/2}} g_s^3(\bar{\mu}) [1 + \mathcal{O}(g_s^2)] , \quad (32)$$

$$= -\frac{5}{(4\pi)^3} (9-n_f)(1+n_f/6) \left(\frac{g_E^2}{m_E} \right)^3 \left[1 + \mathcal{O} \left(\left(\frac{g_E^2}{m_E} \right)^2 \right) \right] . \quad (33)$$

The more conservative approach in the resummations based on EQCD expansion (27) should be to resum separately the expansion of terms which are powers of g_E^2/m_E and the expansion of terms which are powers of $\lambda_E^{(1)}/m_E$, because the two expansions represent probably two topologically different families of diagrams. The problem with the latter expansion is that we know only the leading term there, which is written in terms of the QCD coupling parameter $g_s(\bar{\mu})$ in Eq. (32), and in terms of the first EQCD coupling parameter g_E^2/m_E in Eq. (33). The latter equation, in comparison to the former, represents some kind of (EQCD-)resummation of the $\lambda_E^{(1)}/m_E$ -family of terms. Since the parameters g_E^2/m_E and $\lambda_E^{(1)}/m_E$ are both of the effective EQCD theory, the expression (33) may be considered as better, but less conservative. While $\lambda_E^{(1)}/m_E$ should be independent of the renormalization scale $\bar{\mu} = \mu_M (\sim m_E)$, we will later see that the leading order EQCD expression (33) is significantly less μ_M -dependent than the leading order QCD expression (32), especially when the Padé resummations $P[1/1](a(\mu_M))$ are applied to expansions (28)-(29) for m_E^2 and g_E^2 .

The coupling parameter g_E and the Debye screening mass m_E are physical quantities, and thus they are independent of the renormalization scale ($\bar{\mu}$). This independence is reflected in the coefficients of expansions (28)-(29) in the terms proportional to $\beta_0 \ln \bar{\mu}$. Inserting expansions (28) and (29) into series (27), and using relation (26), leads to an expansion for the sum \tilde{p}_{M+G} in terms of the QED coupling $g_s \equiv g_s(\bar{\mu})$

$$\begin{aligned} \tilde{p}_{M+G} &\equiv \frac{3\pi}{2} \frac{1}{T m_E^3} (p_M + p_G) \\ &= 1 + g_s \frac{3^2}{4\pi} \frac{1}{(1+n_f/6)^{1/2}} \left[-\frac{3}{4} - \ln \left(\frac{\Lambda_E}{2m_E} \right) \right] \\ &\quad + g_s^2 \frac{3^3}{(4\pi)^2} \frac{1}{(1+n_f/6)} \left[-\frac{89}{24} - \frac{\pi^2}{6} + \frac{11}{6} \ln 2 \right] \\ &\quad + g_s^3 \frac{3}{(4\pi)^3} \frac{1}{(1+n_f/6)^{1/2}} \left\{ K_3 \left[-\frac{3}{4} - \ln \left(\frac{\Lambda_E}{2m_E} \right) \right] \right. \\ &\quad \left. + \frac{3^3}{(1+n_f/6)} \left[8(\alpha_M + \alpha_G) \ln \left(\frac{\Lambda_E}{2m_E} \right) + 8 \alpha_G \ln \left(\frac{m_E}{3g_E^2} \right) + \beta_M + \delta_G \right] \right. \\ &\quad \left. - \frac{5}{3} (9-n_f) + 12\beta_0 \ln \left(\frac{\bar{\mu}}{2\pi T} \right) \left[-\frac{3}{4} - \ln \left(\frac{\Lambda_E}{2m_E} \right) \right] \right\} + \mathcal{O}(g_s^4) , \end{aligned} \quad (34)$$

where the constant K_3 is

$$K_3 = \frac{1}{12} \frac{1}{(1+n_f/6)} (-99.9089 - 35.1402 n_f - 7.08145 n_f^2) . \quad (35)$$

The dependence on the factorization scale Λ_M in the expansion (34) disappeared as it should. Further, the quantity p_{M+G} is independent of the renormalization scale $\bar{\mu}$, and this is reflected by the term proportional to $\beta_0 \ln \bar{\mu}$ in the coefficient at g_s^3 in Eq. (34).

We note that the only unknown dimensionless coefficient in (34) is δ_G which, as argued before, is expected to be $|\delta_G| \sim 1$.

The knowledge of the expansion of the short-distance pressure p_E is less complete – this is an expansion in powers of g_s^2 , and it is known only up to $\sim g_s^4$ (cf. Ref. [3]). However, important parts of the coefficient at g_s^6 in p_E can be deduced from the requirement of $\bar{\mu}$ -independence of p_E and of the Λ_E -independence of p_{E+M+G} (Λ_E is the factorization scale for the sum $p_E + p_{M+G}$). After some (tedious) algebra, we end up with the following expansion of p_E up to $\sim g_s^6$:

$$p_E(T) = p_{\text{ideal}}(T) \left[1 - \frac{15}{4} \frac{(1+5n_f/12)}{(1+21n_f/32)} R_E^{\text{can}}(T) \right] , \quad (36)$$

where

$$p_{\text{ideal}}(T) = \frac{8\pi^2}{45} T^4 \left(1 + \frac{21}{32} n_f \right), \quad (37)$$

$$\begin{aligned} R_{\text{E}}^{\text{can}}(T) = & \left(\frac{g_s}{2\pi} \right)^2 \left\{ 1 + \left(\frac{g_s}{2\pi} \right)^2 \left[2\beta_0 \ln \left(\frac{\bar{\mu}}{2\pi T} \right) - 36 \frac{(1+n_f/6)}{(1+5n_f/12)} \ln \left(\frac{\Lambda_{\text{E}}}{\kappa T} \right) \right] \right. \\ & + \left(\frac{g_s}{2\pi} \right)^4 \left[4\beta_0^2 \ln^2 \left(\frac{\bar{\mu}}{2\pi T} \right) + 2 \ln \left(\frac{\bar{\mu}}{2\pi T} \right) \left(\beta_1 - 72\beta_0 \frac{(1+n_f/6)}{(1+5n_f/12)} \ln \left(\frac{\Lambda_{\text{E}}}{\kappa T} \right) \right) \right. \\ & \left. \left. + \frac{36}{(1+5n_f/12)} \ln \left(\frac{\Lambda_{\text{E}}}{\kappa T} \right) \left(-\frac{1}{2}(1+n_f/6)(3P_m(n_f) + K_3/6) + 18(\alpha_{\text{M}} + \alpha_{\text{G}}) \right) + \delta_{\text{E}} \right] + \mathcal{O}(g_s^6) \right\}, \quad (38) \end{aligned}$$

and the parameter κ was introduced such that the NLO coefficient is made up of only two logarithmic terms proportional to $\ln(\bar{\mu}/2\pi T)$ and $\ln(\Lambda_{\text{E}}/\kappa T)$ as shown above

$$\ln \left(\frac{2\pi}{\kappa} \right) = \frac{1}{135} \frac{1}{(1+n_f/6)} (244.898 + 17.2419 n_f - 0.415029 n_f^2). \quad (39)$$

For example, $\kappa \approx 1.0241, 1.47922$ for $n_f = 0, 3$, respectively. At order g_s^6 in expansion (38), only the dimensionless number δ_{E} is unknown – it is independent of the energy scales and of their ratios, just like δ_{G} . We organized the coefficient at g_s^6 in Eq. (38) in the following way: the $\bar{\mu}$ -dependent terms are written in powers of $\ln(\bar{\mu}/2\pi T)$; the IR cutoff (Λ_{E})-dependent terms are written in terms of $\ln(\Lambda_{\text{E}}/\kappa T)$, because this combination absorbs all the $\ln(\bar{\mu}/2\pi T)$ -independent terms in the coefficient at g_s^4 . It is reasonable to expect that the $\ln(\bar{\mu}/2\pi T)$ -independent terms at $\sim g_s^6$ would also be absorbed to a large degree by a quantity proportional to the combination $\ln(\Lambda_{\text{E}}/\kappa T)$. That's why we expect the number δ_{E} to be small. A conservative expectation would be that $|\delta_{\text{E}}|$ is not larger than the $\ln(\Lambda_{\text{E}}/\kappa T)$ -term there:

$$-|k_2^{(0)}(\Lambda_{\text{E}})| < \delta_{\text{E}} < +|k_2^{(0)}(\Lambda_{\text{E}})|, \quad (40)$$

where

$$k_2^{(0)}(\Lambda_{\text{E}}) \equiv \frac{36}{(1+5n_f/12)} \ln \left(\frac{\Lambda_{\text{E}}}{\kappa T} \right) \left(-\frac{1}{12} K_3(1+n_f/6) + 18(\alpha_{\text{M}} + \alpha_{\text{G}}) - \frac{3}{2}(1+n_f/6)P_m(n_f) \right). \quad (41)$$

While δ_{E} is independent of any scale, $k_2^{(0)}$ will have only slight dependence on temperature T when we will take $\Lambda_{\text{E}} = \sqrt{2\pi T m_{\text{E}}(T)}$ ($\sim g_s^{1/2} T$). This choice of Λ_{E} was taken also in Ref. [21].

III. NUMERICAL ANALYSIS OF UNPHYSICAL DEPENDENCE ON SCALES

Expansions (34) or (27) for $p_{\text{M+G}}$, and (36)-(38) for p_{E} , in conjunction with expansions (28) and (29) for m_{E}^2 and g_{E}^2 , will form the basis of our numerical analysis. The only unknown parameters are δ_{G} and δ_{E} which will be allowed to vary in the intervals (21) and (40). The numerical analysis will be performed in analogy with that of our previous work [21]. There, expansion corresponding to present Eq. (34) for $\tilde{p}_{\text{M+G}}$ was applied but contained only terms up to $\sim g_s^2$; expansion for $R_{\text{E}}^{\text{can}}$ of present Eq. (38) contained only terms up to $\sim g_s^4$; and expansion (29) only the leading term. The resummations in Ref. [21] were performed with Padé approximants, or with simple evaluation of the truncated perturbation series (TPS). In the present work, the resummations will be performed with Padé, Borel-Padé (cf. Appendix A), or TPS.

As argued in the Introduction and in Ref. [21], the $\overline{\text{MS}}$ renormalization scale $\bar{\mu}$ should be chosen accordingly in different regimes for the resummation of the different quantities (34), (38), and (28)-(29). The scale regime for $\bar{\mu}$ should be of the order of a typical physical scale that corresponds to the quantity to be resummed. Therefore, the renormalization scale $\bar{\mu} \equiv \mu_{\text{E}}$ in the short-distance quantity (38) is $\mu_{\text{E}} \sim 2\pi T$. For the long-distance EQCD quantities (28)-(29), the relevant scale is $\bar{\mu} \equiv \mu_m$ such that $\mu_m \sim m_{\text{E}}$ ($\sim g_s T$). For the long-distance quantity $p_{\text{M+G}}$, Eqs. (34) and (27), the relevant scale $\bar{\mu} \equiv \mu_{\text{M+G}}$ should be somewhere between $\sim g_s T$ and $g_s^2 T$; we will take it $\sim g_s T$, i.e., $\bar{\mu} = \mu_{\text{M}} \sim g_s T$. Unless otherwise stated, we will take $\mu_{\text{M}} = \mu_m = m_{\text{E}}(\mu_m)$. For the factorization scale Λ_{E} we take, unless otherwise stated, the geometric mean between the hard scale $2\pi T$ and the EQCD scale m_{E} : $\Lambda_{\text{E}} = [2\pi T m_{\text{E}}]^{1/2}$ ($\sim g_s^{1/2} T$). For m_{E}^2 and g_{E}^2 we will take, unless otherwise stated, the P[1/1](a) Padé approximant (PA) with respect

to a (cf. Appendix A), where $a \equiv a(\bar{\mu}) \equiv (g_s(\bar{\mu})/2\pi)^2$ and the scale $\bar{\mu}$ ($\equiv \mu_m$) is adjusted so that $\bar{\mu} = m_E$. We will see below that $P[1/1](a)$ is a very reasonable resummation for m_E^2 .

Further, if not stated otherwise, we will take for the number of active (and massless) quark flavors $n_f = 3$. For the QCD coupling parameter $\alpha_s(\bar{\mu}) \equiv g_s^2(\bar{\mu})/(4\pi)$ we take the reference value $\alpha_s(m_\tau^2, \overline{\text{MS}}) = 0.334$ which is approximately the value extracted from the hadronic τ decay data [36, 37]. We work in the $\overline{\text{MS}}$ scheme and use for the β function $P[2/3](a)$ Padé approximant (PA) ($a = \alpha_s/\pi$), unless otherwise stated. This approximant, as shown in Refs. [17], represents a reasonable (quasi)analytic continuation of the TPS of $\beta_{\overline{\text{MS}}}(a)$ into the regime of large a [with $\bar{\mu}$ down to $\alpha_s(\mu) \approx 1.0$] where the TPS is practically inapplicable.

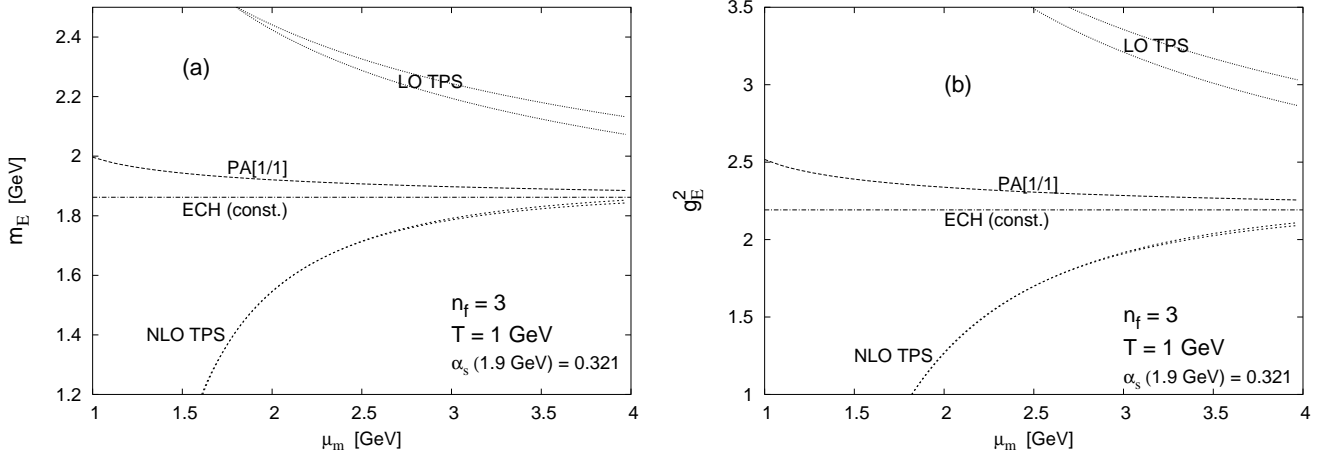


FIG. 1: (a) The Debye screening mass m_E , and (b) the EQCD coupling parameter g_E^2 , as functions of the renormalization scale μ_m , when $T = 1$ GeV. The upper of the LO TPS (NLO TPS) twin curves has $a(\mu_m^2)$ evolved by the one-loop (two-loop) RGE from $a(m_\tau^2)$. The other curves have $a(\mu_m^2)$ evolved by the four-loop PA [2/3] beta function.

First, the resummation of the expansion of the squared Debye screening mass m_E^2 (28) and of the EQCD coupling parameter g_E^2 (29), respectively, are performed. Both expansions are next-to-leading order (NLO) in $a(\mu_m) = [g_s(\mu_m)/2\pi]^2$. Therefore, the diagonal $P[1/1](a)$ can be constructed and should be a good candidate. Figs. 1(a) and 1(b) show the results, as a function of the renormalization scale μ_m ($\sim m_E$). The values of m_E in Fig. 1(a) are obtained by the corresponding resummation of expansion (28) for m_E^2 and then taking the square root. In addition to $P[1/1](a(\mu_m))$, also the effective charge method result (ECH) [38, 39, 40], as well as the TPS results, are presented. The ECH result is the NLO TPS at a specific value of the renormalization scale, so it is automatically independent of μ_m . We see from Figs. 1(a) and 1(b) that PA's $P[1/1](a)$ for m_E^2 and g_E^2 are very good approximations as they almost eliminate μ_m -dependence contrary to the TPS-expressions which show (both for LO and NLO) a very strong unphysical μ -dependence. This is in accordance with Ref. [12] where it is argued that any diagonal $P[n/n](a(\mu))$ of a QCD observable has significantly reduced μ -dependence, i.e., it is μ -independent in the large- β_0 limit.⁴ As mentioned before, we will choose the mass m_E by the condition $(m_E^2)^{P[1/1]} = \mu_m^2$, and we will denote the square root of this value as $m_E^{(0)}(T)$

$$(m_E^2(T))^{P[1/1]} = \mu_m^2 \equiv \left(m_E^{(0)}(T)\right)^2. \quad (42)$$

At $T = 1$ GeV (and $n_f = 3$), this value is $m_E^{(0)} \approx 1.923$ GeV.⁵

In Figs. 2 we present the short-distance pressure p_E as a function of the respective renormalization scale μ_E – various resummed expressions based on the perturbation series (36)-(38) in powers of $a(\mu_E) = [g_s(\mu_E)/2\pi]^2$, for $T = 1$ GeV and $\delta_E = 0$. The naming of each resummation refers to the use of the corresponding approximant for R_E^{can} in p_E of Eq. (36) as a function of $a(\mu_E) = [g_s(\mu_E)/2\pi]^2$. For example, $P[2/1]$ means that we apply to the perturbation series (38) in powers of $a(\mu_E)$ the Padé approximant $P[2/1](a(\mu_E))$; $BP[1/2]$ means that we apply $P[1/2]$ to the

⁴ There exists an extension of the diagonal PA's such that it is completely μ -independent [16], or μ - and scheme-independent [17].

⁵ Fig. 1(a) was presented in our previous work [21], but there the curves are slightly lower (by about 0.02 GeV) due to inadvertent omission of the factor $(1 + n_f/6)^{-1}$ appearing in our Eq. (30) for P_m .

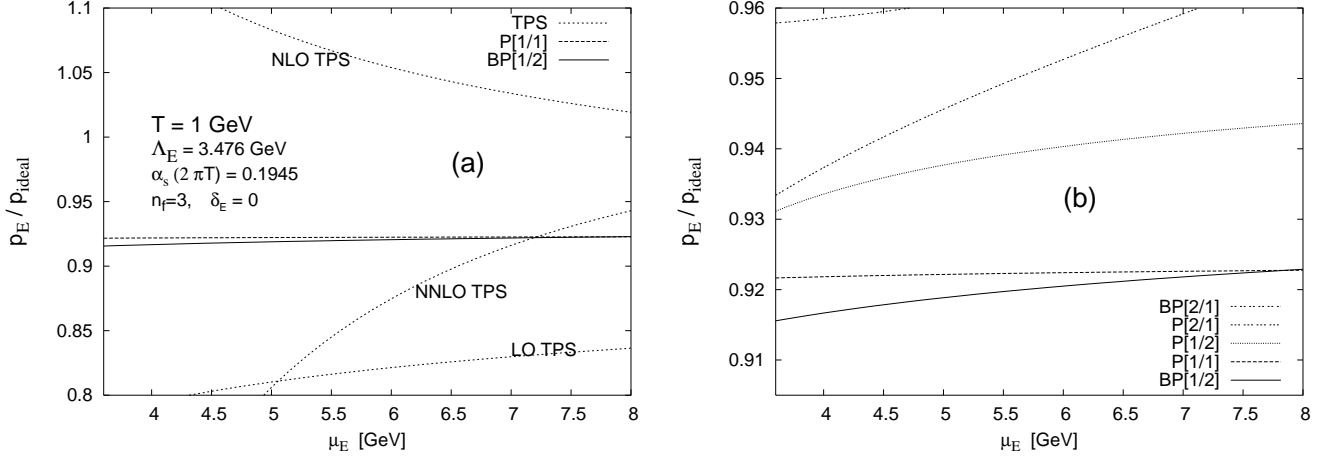


FIG. 2: The short-distance pressure p_E , at $T = 1$ GeV, as a function of the corresponding renormalization scale μ_E – various approximants are applied to the perturbation expansion (38) in powers of $a(\mu_E) = [g_s(\mu_E)/2\pi]^2$, and $\delta_E = 0$ was taken. Figure (b) has a finer vertical scale and includes some approximants not shown in Fig. (a).

Borel transform of expansion (38) – cf. Appendix A. The range of μ_E is around $2\pi T$, i.e., the order of the relevant physical modes contributing to p_E . Further, the IR cutoff Λ_E is taken fixed: $\Lambda_E = [2\pi T m_E^{(0)}(T)]^{1/2}$. The results are normalized by $p_{\text{ideal}} = (8\pi^2/45)(1 + 21n_f/32)$, i.e., the expression for the pressure when $T \rightarrow \infty$ [cf. Eq. (36)]. From Fig. 2(a) we see that the TPS's are not acceptable, due to too strong μ_E -dependence. For the same reason, as seen from Fig. 2(b), the approximants P[1/2], P[2/1], and Borel-Padé BP[2/1] are not acceptable. The only acceptable candidates are P[1/1], and BP[1/2]. We note that P[1/1] is based explicitly only on the NLO series (up to $\sim a^2$) of Eq. (38). Nonetheless, we will include later P[1/1] of R_E^{can} in some of our results, because it is close to BP[1/2] and is very stable under variation of μ_E (NL ECH also gives values close to P[1/1] and BP[1/2]). Although the results are presented only for the case $T = 1$ GeV and $\delta_E = 0$, the behaviour and the conclusions remain the same for other temperatures, and for other values of δ_E in the interval (40).

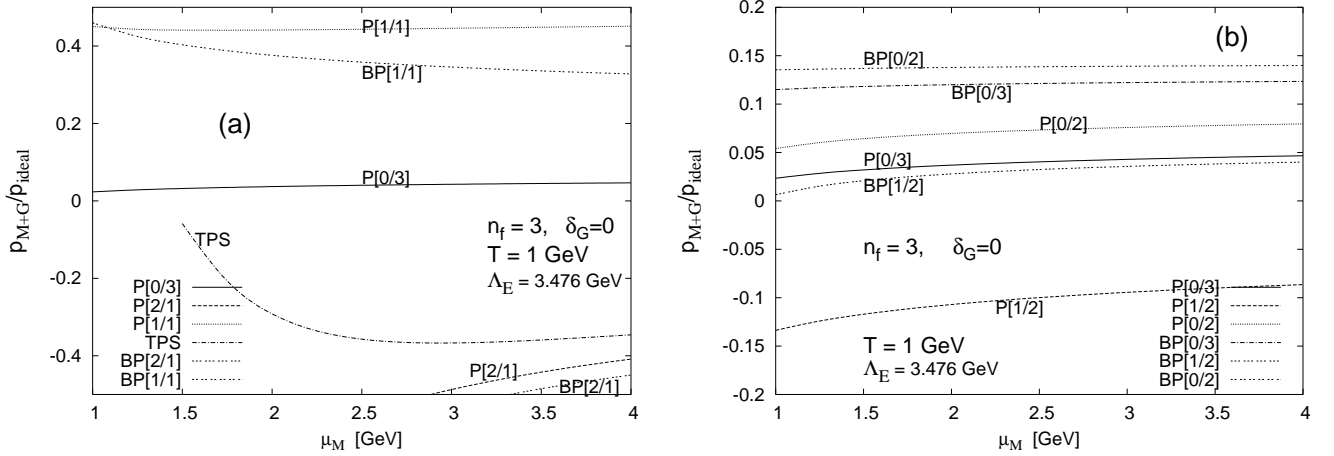


FIG. 3: The long-distance pressure p_{M+G} , at $T = 1$ GeV, as a function of the corresponding renormalization scale μ_M – various approximants are applied to the perturbation expansion (34) in powers of $g_s(\mu_M)$, and $\delta_G = 0$ was taken. Figure (b) has a finer vertical scale and includes some approximants not shown in Fig. (a).

Similar analysis is now performed for the long-distance pressure p_{M+G} . Padé and Borel-Padé resummations are first applied to expansion (34) for $\tilde{p}_{M+G} (\propto p_{M+G}/m_E^3)$ which starts with one and is in powers of $g_s(\mu_M)$ – cf. Appendix A for more details. In Figs. 3 we present the results of various resummations as a function of the respective renormalization scale μ_M , for $T = 1$ GeV and $\delta_G = 0$. The factor m_E^3 in the first line of Eq. (34) was taken with P[1/1] for $m_E^2(\mu_m)$, with the renormalization scale $\mu_m = \mu_M$. The UV cutoff Λ_E was taken fixed according to the formula: $\Lambda_E = (2\pi T m_E^{(0)})^{1/2}$. The TPS and some of the other resummations show significant μ_M -dependence. Further, BP[0/2] and P[0/2] are of

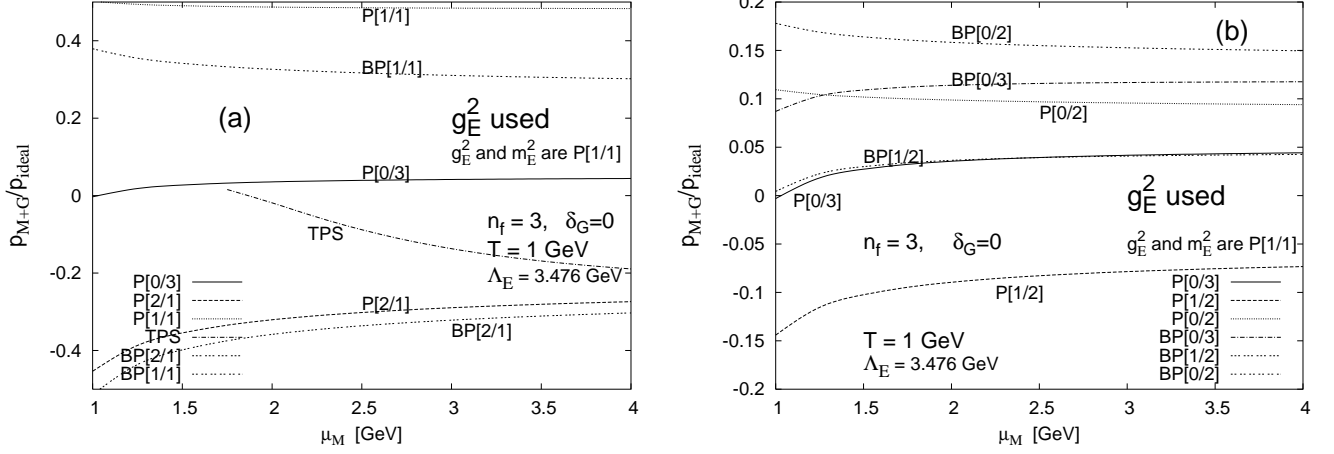


FIG. 4: Same as in Figs. 3, but now \tilde{p}_{M+G} is based on expansion (27) in g_E^2/m_E . Details are given in the text.

lower order (NNLO) and do not take explicitly into account the numerically important $\sim g_s^3$ terms of expansion (34) of \tilde{p}_{M+G} ($\sim g_s^6$ in p_{M+G}). We decide at this stage to consider only the N³LO resummations: P[1/2], P[0/3], BP[1/2], and BP[0/3]. The approximant P[0/2](g_s) for $\tilde{p}_{M(+G)}$ was considered in our previous work [21], and we include it later in Figs. 7 and 9 in the presentation of $p(T)$. The conclusions of this paragraph survive when other values of T and δ_G are used.

We alternatively apply our resummation procedure to the EQCD expansion (27) instead of (34) for \tilde{p}_{M+G} . The results are presented in Figs. 4. The values of g_E^2 and m_E^2 in (27) are chosen as P[1/1]($a(\mu_m)$), due to their μ_m -stability ($\mu_m = \mu_M$ taken) as seen in Figs. 1, and then Padé or Borel-Padé are applied to expansion (27) in powers of the EQCD parameter g_E^2/m_E ($\sim g_s$), without the $\lambda_E^{(1)}/m_E$ -term which is then added separately as the leading order QCD term $\propto g_s^3(\mu_M)$, Eq. (32). When Padé or Borel-Padé based on TPS terms of order lower than $\sim g_s^3$ for \tilde{p}_{M+G} of Eq. (27) are applied – such as P[1/1], BP[1/1], P[0/2] or BP[0/2] to TPS (27) of \tilde{p}_{M+G} – the $\lambda_E^{(1)}/m_E$ -term is not included and not added as it represents a term $\sim g_s^3$ of \tilde{p}_{M+G} ($\sim g_s^6$ to p_{M+G}). The TPS curve in Fig. 4(a) was obtained by evaluating expansion (27) of \tilde{p}_{M+G} directly as EQCD TPS, with the values for g_E^2 and m_E^2 taken as simple (NLO) TPS's (28)-(29) at $\bar{\mu} = \mu_M$. The conclusions from Figs. 4 are the same as in the procedure leading to Figs. 3: the N³LO resummations P[1/2], P[0/3], BP[1/2], and BP[0/3] all remain acceptable candidates at this stage, and this conclusion turns out to be independent of T and δ_G .

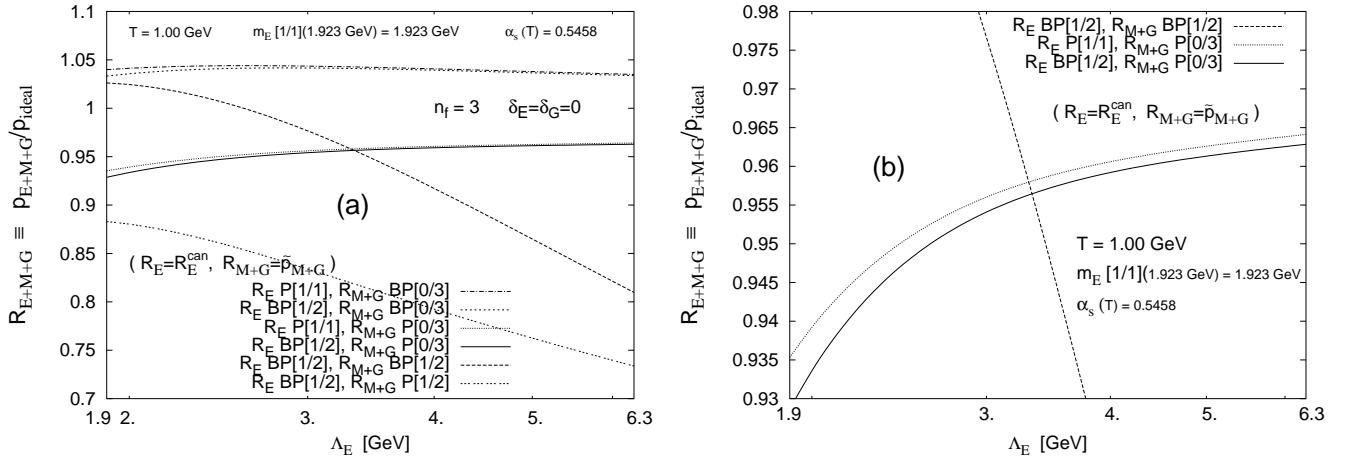


FIG. 5: The total pressure $p_{\text{QCD}} = p_E + p_{M+G}$, at $T = 1$ GeV, as a function of the corresponding factorization scale Λ_E – various approximants are applied separately to the perturbation expansions $R_E^{\text{can}}(a(\mu_E))$ (38) and $\tilde{p}_{M+G}(g_s(\mu_M))$ (34). Details are given in the text. Figure (b) has a finer vertical scale.

Another necessary condition for an acceptable resummation is that the spurious Λ_E -dependence in the total sum $p_E + p_{M+G}$ be weak. In Figs. 5 we present the results on Λ_E -dependence, at $T = 1$ GeV, combining various aforementioned

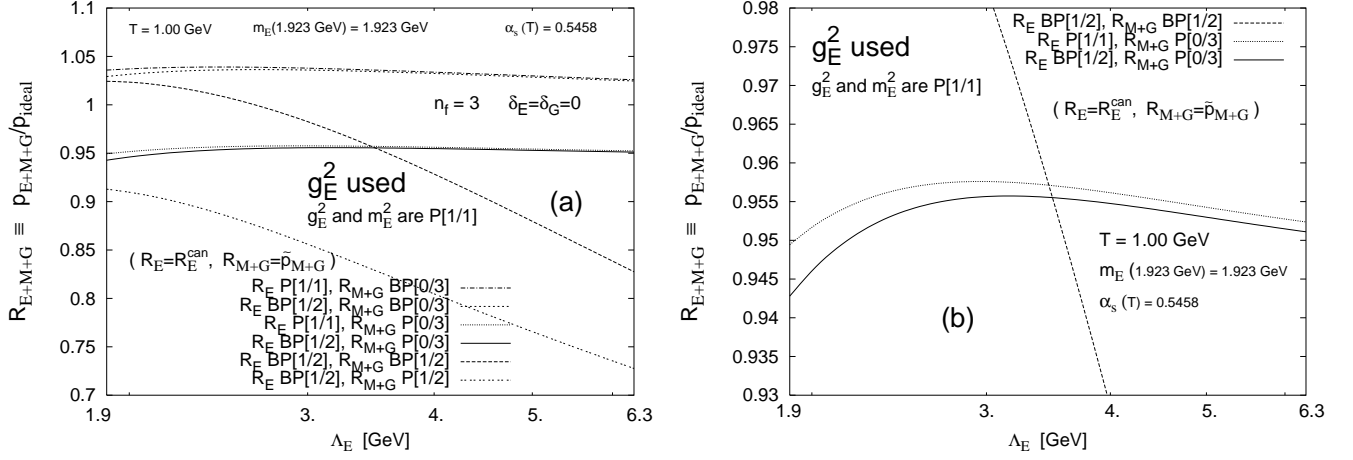


FIG. 6: Same as in Figs. 5, but now \tilde{p}_{M+G} is based on expansion (27) in g_E^2/m_E . Further details are given in the text.

resummations for p_E and p_{M+G} that were found acceptable so far. Here, $m_E = m_E^{(0)}$ was fixed in the aforementioned way (42), $\mu_E = 2\pi T$, and $\mu_M = \mu_m = m_E^{(0)}$. Now, $\Lambda_E \neq \sqrt{\mu_E \mu_M}$, but varies between μ_M (≈ 1.9 GeV) and μ_E (≈ 6.3 GeV). The two unknown parameters were chosen to be $\delta_E = \delta_G = 0$. We see that the curves with P[0/3] and B[0/3] used for \tilde{p}_{M+G} have acceptably weak Λ_E -dependence, while those with P[1/2] and BP[1/2] used for \tilde{p}_{M+G} have unacceptably strong Λ_E -dependence. Thus, we are left with just two types of resummations which fulfill the necessary conditions of weak μ_E , μ_M and Λ_E dependence:

1. P[0/3]($g_s(\mu_M)$) for \tilde{p}_{M+G} ; and either P[1/1]($a(\mu_E)$) or BP[1/2]($a(\mu_E)$) for $R_E^{\text{can}}(a(\mu_E))$;
2. BP[0/3]($g_s(\mu_M)$) for \tilde{p}_{M+G} ; and either P[1/1]($a(\mu_E)$) or BP[1/2]($a(\mu_E)$) for $R_E^{\text{can}}(a(\mu_E))$.⁶

These conclusions do not change when the values of T , δ_E and δ_G are changed. We note that P[1/1]($a(\mu_E)$) is of lower order and therefore does not use the term $\sim a^3$ in expansion (38).

We can repeat the same analysis, but using expansion (27) for \tilde{p}_{M+G} in powers of (g_E^2/m_E) instead of expansion (34) in powers of $g_s(\mu_M)$. The values of g_E^2 and m_E^2 are taken as P[1/1]($a(\mu_M)$), with $\mu_M = \mu_m = m_E^{(0)}$. The results are given in Figs. 6, they are similar to those of Figs. 5, and the conclusions are the same.

IV. NUMERICAL RESULTS AS A FUNCTION OF TEMPERATURE

We will first concentrate on the first family of resummations, i.e., those with P[0/3] for \tilde{p}_{M+G} . We present the results for these resummations as a function of temperature T in Fig. 7(a), for $\delta_E = \delta_G = 0$, and \tilde{p}_{M+G} is based on expansion (34) in powers of $g_s(\mu_M)$. In addition to these resummations, we include also the same type of resummations where the p_G part is excluded ($p_E + p_M$), where we use in p_M for the IR cutoff: $\Lambda_M = (m_E^{(0)})^2/\Lambda_E$. We use $\mu_E = 2\pi T$; $\mu_M = \mu_m = m_E = m_E^{(0)}(T)$; $\Lambda_E = \sqrt{\mu_E \mu_M}$. We can see in Fig. 7(a) that the presence of p_G , at least for $\delta_G = 0$, decreases the value of the total pressure somewhat. For comparison, we also include the result of resummation of P[1/1] for R_E^{can} and P[0/2] for \tilde{p}_M (cf. Ref. [21]), i.e., the case where the terms $\sim g_s^3$ in \tilde{p}_{M+G} (terms $\sim g_s^6$ in p_{M+G}) are not explicitly accounted for (and neither are the terms $\sim g_s^6$ in p_E). Fig. 7(a) shows one interesting feature: when the terms $\sim g_s^6$ in p_{M+G} are explicitly accounted for in the resummation, the sign of the curvature becomes negative in the entire temperature interval – i.e., at least there where the resummation is applicable: $T > 0.3$ GeV. Thus the curvature at low temperatures has now the same sign as suggested by the known relation $p/p_{\text{ideal}} \ll 1$ at $T \sim T_c \approx 0.2$ GeV (see later in this Section). For $T < 0.3$ GeV our resummations cannot be applied any more, because in that case $\mu_m (= \mu_M) < 0.81$ GeV, but the P[2/3](a) beta function does not allow running below such values [$a(\mu_m)$ blows up]. When we vary the values of δ_G and δ_E in the intervals (21) and (40), respectively, the predictions do not change much. This is presented in Fig. 7(b).

⁶ NL ECH could be used instead of P[1/1] or BP[1/2] for R_E^{can} , but the results are similar in all three cases, at any temperature.

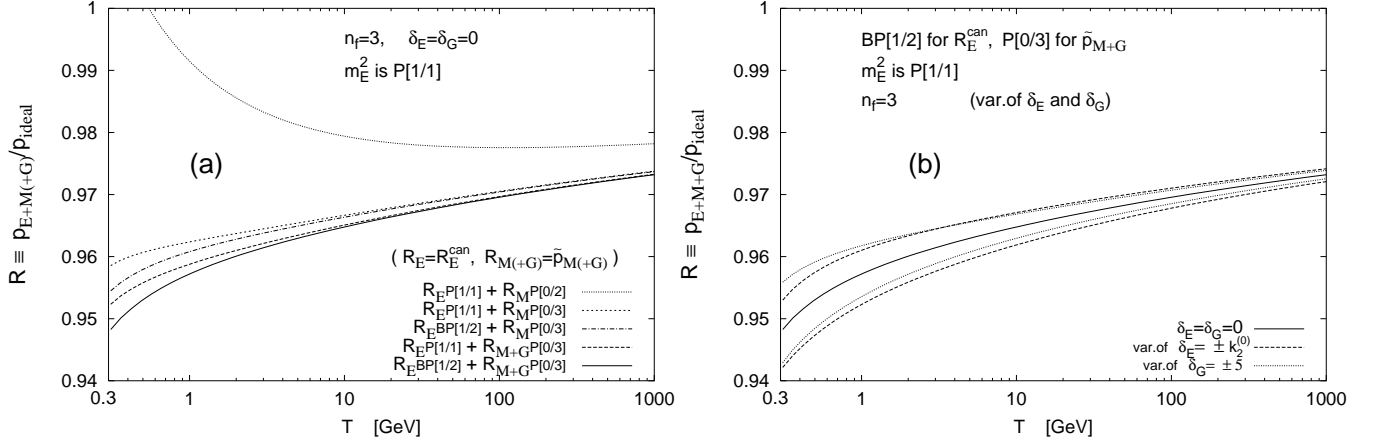


FIG. 7: (a) The total pressure p (normalized by p_{ideal}) as a function of temperature T , with $\delta_E = \delta_G = 0$ – various resummations are applied: for $R_E^{can}(a(\mu_E))$ the approximants $P[1/1](a(\mu_E))$ and $BP[1/2](a(\mu_E))$; for $\tilde{p}_{M+G}(g_s(\mu_M))$ the approximant $P[0/3](g_s(\mu_M))$. Shown are also the analogous results when p_G is excluded. In addition, a resummation which does not account for the $\sim g_s^6$ terms in p_{M+G} is included (dotted line). (b) Variation of a specific Padé/Borel-Padé resummation when the unknown parameters δ_G and δ_E are varied. The full curves in (a) and (b) are the same curves. Further explanations are given in the text.

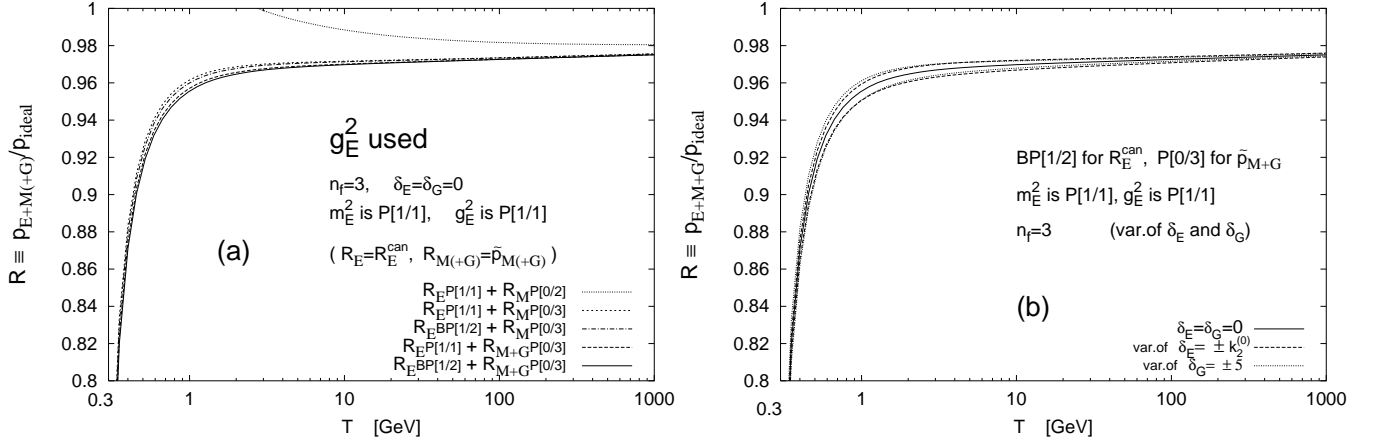


FIG. 8: Same as in Fig. 7, but now \tilde{p}_{M+G} is based on expansion (27) in g_E^2/m_E – using the resummed g_E^2 and m_E^2 as $P[1/1](a(\mu_M))$.

When we do not base the resummations of \tilde{p}_{M+G} on expansion (34) in powers of $g_s(\mu_M)$, but rather on expansion (27) in powers of the EQCD parameter g_E^2/m_E [using the resummed g_E^2 and m_E^2 as $P[1/1](a(\mu_M))$, and adding the $\lambda_E^{(1)}/m_E$ -term separately as the leading order QCD term $\propto g_s^3(\mu_M)$, Eq. (32)], remarkable changes occur for the results of p/p_{ideal} as a function of temperature. The obtained results, analogous to those of Figs. 7(a) and 7(b), are presented in Figs. 8(a) and 8(b), respectively. The “low order” dotted curve in Fig. 8(a) (the uppermost), which does not use information on $\sim g_s^6$ terms (and thus does not include the $\lambda_E^{(1)}$ -term), still does not change the curvature in the low temperature regime. On the other hand, “higher order” Padé resummations of \tilde{p}_{M+G} , which use information on $\sim g_s^6$ terms in p_{M+G} ($\sim g_s^3$ in \tilde{p}_{M+G}) and include, added separately, the $\lambda_E^{(1)}/m_E$ -term in \tilde{p}_{M+G} as the leading order QCD term $\propto g_s^3(\mu_M)$ [Eq. (32)], result in a pronounced negative curvature and a rapid fall of p/p_{ideal} when the temperature falls down toward the critical values $T_c \approx 0.2$ GeV. This behavior is qualitatively correct because we know that it must be $p/p_{ideal} \ll 1$ at $T \approx T_c$ (see later). In that respect, this phenomenon indicates that the resummations of \tilde{p}_{M+G} based on expansion (27) in powers of the effective EQCD theory parameter g_E^2/m_E are more reliable than those based on expansion (34) in powers of g_s . The low- T results of Figs. 8 turn out to be closer to those of lattice calculations, the feature which will be discussed and presented in more detail in Section VI. Another very positive feature can be read off from Fig. 8(b): variation of the Padé and Borel-Padé resummed predictions, when the unknown parameters δ_G and δ_E are varied in the generously wide intervals (21) and (40), is weak.

Now we turn to the second family of resummations, i.e., those with $BP[0/3]$ for \tilde{p}_{M+G} instead of $P[0/3]$. We present

these results, as a function of temperature T , with values of δ_E and δ_G varied in the intervals (40) and (21), in Figs. 9(a) and 9(b). In Fig. 9(a), BP[0/3] was applied to expansion (34) for \tilde{p}_{M+G} ; in Fig. 9(b) to expansion (27)

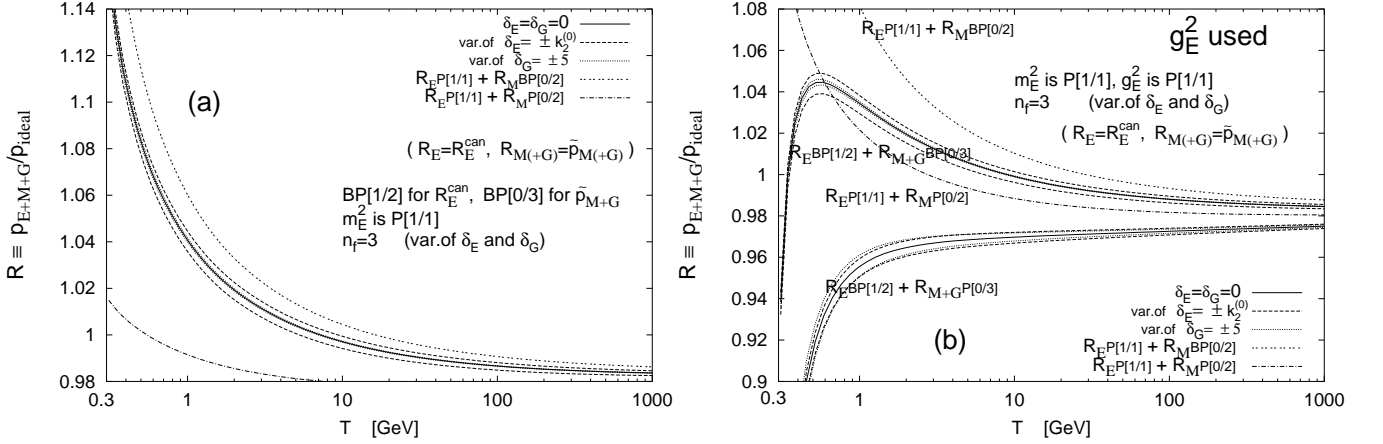


FIG. 9: (a) The total pressure \tilde{p} (normalized by p_{ideal}) as a function of temperature T , for various values of δ_E and δ_G , when BP[0/3] is applied to expansion (34) for \tilde{p}_{M+G} (and BP[1/2] to R_E^{can}); (b) Same as in (a), but BP[0/3] for \tilde{p}_{M+G} is based on expansion (27) in g_E^2/m_E , using the resummed g_E^2 and m_E^2 as P[1/1]($a(\mu_M)$).

for \tilde{p}_{M+G} without the $\lambda_E^{(1)}/m_E$ -term, the latter was taken as the leading order $\propto g_s^3(\mu_M)$ of QCD expansion (32) and added separately (only in the “higher order” P[0/3] and BP[0/3] cases). Further, the other parameters and procedures are the same as in Figs. 7-8. For comparison, the lower order counterpart, i.e., with BP[0/2] for \tilde{p}_{M+G} (and P[1/1] for R_E^{can}) is included in these Figures. In addition, for comparison, the corresponding curves when P[0/3] is applied for \tilde{p}_{M+G} , and at lower order P[0/2], are included whenever visible⁷ – see also Figs. 7-8. We observe from Figs. 9 and 7-8 that the choice BP[0/3] for p_{M+G} gives $p/p_{ideal} > 1$ for most of the low temperatures T , and the choice P[0/3] for p_{M+G} gives $p/p_{ideal} < 1$.

We recall that BP[0/3] for \tilde{p}_{M+G} was equally acceptable as P[0/3], when only the demand for weak renormalization and factorization scale dependence is used as a criterion, Figs. 3-6. However, there are several indications (not using the approximate knowledge of the low-temperature curves of p/p_{ideal} from lattice calculations) that the choice BP[0/3] is less acceptable than P[0/3]. Some of them are due to general physical considerations, others are connected with the specific numerical approximation techniques applied here.

Physical considerations provide at least two arguments for expecting $p/p_{ideal} < 1$ and, consequently, for favoring the choice P[0/3]:

1. From the physical point of view one would expect that the pressure of a (relativistic) quark-gluon gas gets lowered relative to the free particle case once the interaction is switched on, simply because we expect that the behavior of interacting massless quarks and gluons is approximately described by (almost free) massive quasi-particles, the mass stemming from Debye screening. Such a behavior is manifest not only within a non-relativistic electromagnetic plasma (calculated according to Debye-Hückel), but shows up also in specific model calculations for a relativistic plasma [6, 7]. Therefore, we expect that $p/p_{ideal} < 1$ for T close to critical temperatures T_c ($\approx 0.15 - 0.25$ GeV).
2. The same qualitative behavior is inferred from a thermodynamic consideration [41]: We know that the pressure (considered as a function of T) remains continuous at the phase transition point $T = T_c$. But below T_c the system is a hadron (mostly pion) gas, which to a good approximation can be described by an ideal pion gas. The corresponding pressure is

$$p_\pi = 3 \frac{\pi^2}{90} T^4 = \frac{3}{16} \frac{8\pi^2}{45} T^4 \quad (T < T_c)$$

⁷ It is natural to regard P[0/2] and P[0/3] (for \tilde{p}_{M+G}) as part of a sequence of approximations, and BP[0/2] and BP[0/3] as part of another sequence of approximations – e.g., Ref. [11] and Figs. 9(a) and 9(b).

TABLE I: The exact and predicted coefficients r_j of the expansion (34) for \tilde{p}_{M+G} in powers of $g_s(\mu_M)$. The scales are fixed as usual: $\mu_M = \mu_m = m_E^{(0)}$ of Eq. (42), $\Lambda_E = (2\pi T m_E^{(0)})^{1/2}$. The temperatures are $T = 1$ GeV and 0.5 GeV; $n_f = 3$. The results $r_3(\delta_G)$ are given for the values $\delta_G = 0 \pm 5$ Eq. (21).

T [GeV]	r_1 (exact)	r_2 (exact)	$r_3(\delta_G)$ (exact)	r_3 (pred. P[0/2])	r_3 (pred. BP[0/2])
1.0	-0.3794	-0.4654	-0.0643 ± 0.1111	0.4077	1.387
0.5	-0.3374	-0.4654	-0.0852 ± 0.1111	0.3524	1.172

TABLE II: The exact and predicted coefficients r_j^{eff} of the expansion (27) for \tilde{p}_{M+G} in powers of the EQCD parameter g_E^2/m_E , without the $\lambda_E^{(1)}$ -term. All the other parameters as in Table I.

T [GeV]	r_1^{eff} (exact)	r_2^{eff} (exact)	$r_3^{\text{eff}}(\delta_G)$ (exact)	r_3^{eff} (pred. P[0/2])	r_3^{eff} (pred. BP[0/2])
1.0	-0.4647	-0.6980	-0.1645 ± 0.2041	0.7490	2.548
0.5	-0.4132	-0.6980	-0.1902 ± 0.2041	0.6474	2.154

which is much smaller than the pressure for an ideal gas of quarks (with n_f flavours) and gluons, Eq. (37). Consequently, the true pressure of the interacting plasma at temperature $T \gtrsim T_c$ (but close to T_c) must be much smaller than the ideal gas value at the same temperature, and we again obtain $p/p_{\text{ideal}} < 1$ for $T \gtrsim T_c$.

From Fig. 9(a) it is seen that $p/p_{\text{ideal}} > 1$ above T_c and even seems to increase when $T \rightarrow T_c$ if the approximant BP[0/3] is applied to expansion (34) of \tilde{p}_{M+G} (g_E^2 not being used/resummed), whereas P[0/3] is in accordance with the aforementioned expectation that $p/p_{\text{ideal}} < 1$ [Fig. 7(a)]. On the other hand, when expansion (27) is used as the basis for resummation (with g_E^2 resummed), p/p_{ideal} falls below one for temperatures very close to T_c even in the case BP[0/3] (but g_E^2 resummed), but it is still larger than 1 for a considerable temperature region above but not far from T_c [Fig. 9(b)]. This indicates that using expansion (27) instead of (34) gives in general more realistic results.

Numerical considerations provide at least two other arguments in favor of the choice P[0/3] for p_{M+G} :

1. If BP[0/3] for \tilde{p}_{M+G} gave results closer to the true values of p_{M+G} than P[0/3], then Fig. 9(b) would suggest that the lower order counterpart P[0/2] (to P[0/3]) for \tilde{p}_{M+G} gives results which lie closer to the true values of p_{M+G} than those from P[0/3] for $T > 0.5$ GeV – a situation that has to be regarded as unlikely.⁸
2. The $\mathcal{O}(g_s^3)$ terms of \tilde{p}_{M+G} predicted by re-expansion of BP[0/2] are clearly worse than those predicted by P[0/2], cf. Tables 1 and 2. This suggests for the respective higher order approximants BP[0/3] and P[0/3] the corresponding hierarchy of reliability.

For all these reasons, we will regard as the acceptable resummation at the $\mathcal{O}(g_s^6)$ level to be the one using P[0/3] for \tilde{p}_{M+G} , and BP[1/2] for R_E^{can} . Further, as mentioned before, the resummation of \tilde{p}_{M+G} appears to be more consistent with the physical expectation of $p/p_{\text{ideal}} < 1$ at $T \rightarrow T_c$ when it is based on expansion (27) of \tilde{p}_{M+G} in powers of the EQCD parameter g_E^2/m_E (with the $\lambda_E^{(1)}/m_E$ -term added separately).

Up until now, all the results presented were for $n_f = 3$. In Figs. 10 we present comparison of (Borel-)Padé predictions in the cases $n_f = 0$ and $n_f = 3$: in Fig. 10(a) when \tilde{p}_{M+G} is based on expansion (34) in powers of g_s ; and in Fig. 10(b) when \tilde{p}_{M+G} is based on expansion (27) in powers of g_E^2/m_E , with the aforementioned treatment of the $\lambda_E^{(1)}/m_E$ -term. In the latter Figure we also included two curves for the case when the $\overline{\text{MS}}$ β function is taken as TPS instead of P[2/3]($a(\mu)$). We see that the negative curvature at low T survives also in the $n_f = 0$ case. Further, the results for $n_f = 0, 3$ depend only very little on the type of the resummation used for the β -function, even at low T .

We present the main results for p/p_{ideal} as a function of temperature, which are given also in Figs. 8(b) and 10(b), in a detailed form in the low-temperature regime in Figs. 11. In the latter Figures, we present further the variation of the curves when the renormalization scales μ_E , and $\mu_M = \mu_m$ are varied around their central values $2\pi T$ and $m_E^{(0)}(T)$ of Eq. (42) by factors 1.5 and 1/1.5.⁹ The variation of μ_E changes the curves insignificantly.

⁸ Note that the lower order “counterpart” P[1/1] (to BP[1/2]) for R_E^{can} gives, at any temperature, values of p_E very similar to those of BP[1/2] – cf. Figs. 7(a) and 8(a).

⁹ The factorization scale is $\Lambda_E = (2\pi T m_E)^{1/2}$ where m_E is the square root of P[1/1] of $m_E^2(\mu_m)$. Λ_E changes only little with the variation of the scale $\mu_M = \mu_m$.

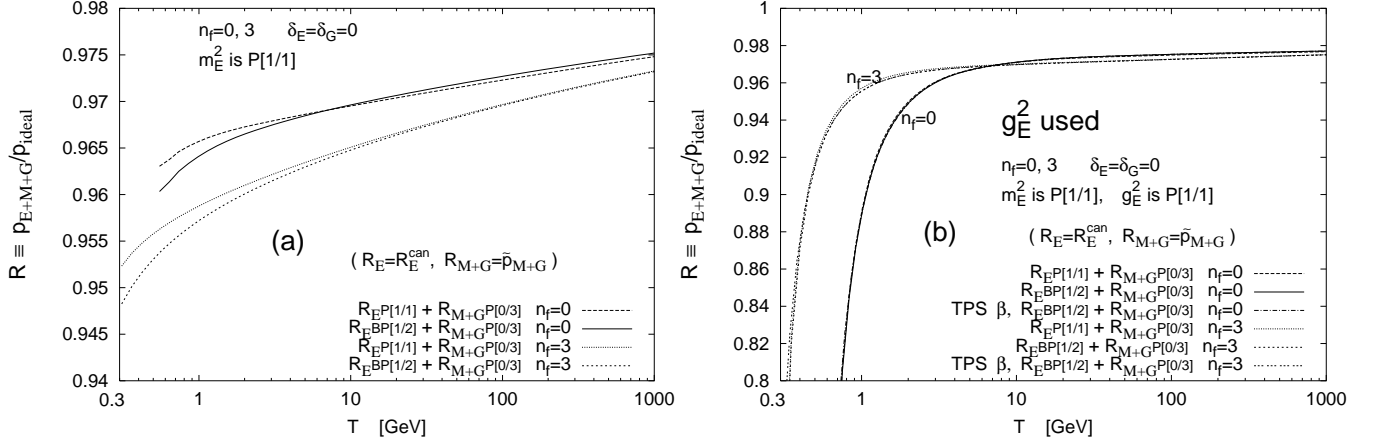


FIG. 10: (a) Analogous to Fig. 7(a), but with $n_f = 0$ for comparison; (b) as in Fig. (a), but now \tilde{p}_{M+G} is based on expansion (27) in g_E^2/m_E – using the resummed g_E^2 and m_E^2 as $P[1/1](a(\mu_M))$, i.e., analogous to Fig. 8(a) but with $n_f = 0$ for comparison.

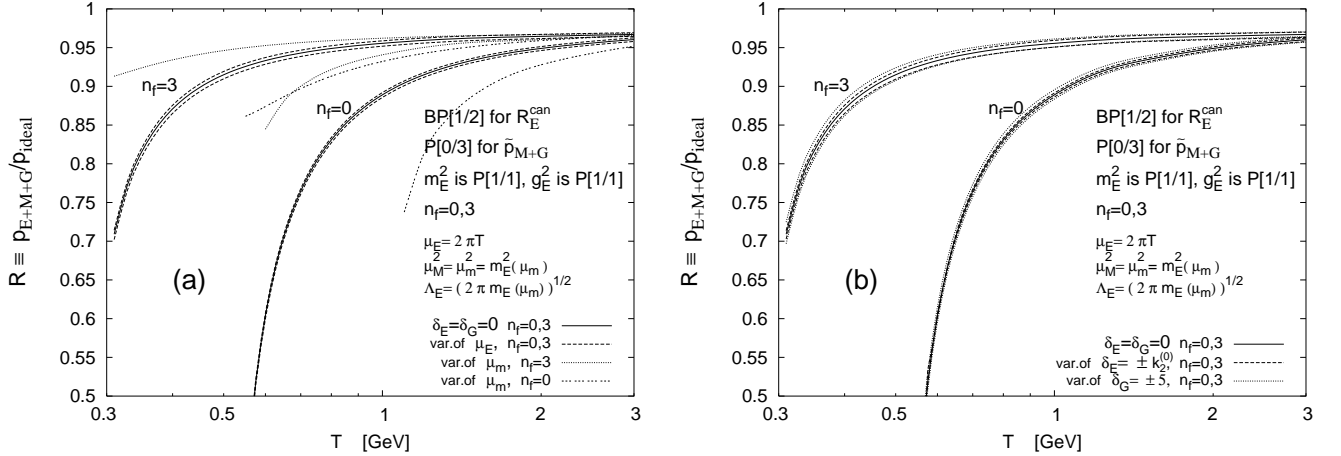


FIG. 11: (a) The pressure p , normalized by p_{ideal} , as a function of temperature T , for the most acceptable resummation approach: $P[0/3]$ for \tilde{p}_{M+G} of expansion (27), and $BP[1/2]$ for R_E^{can} , for $\delta_E = \delta_G = 0$, and $n_f = 3, 0$. The variation of the renormalization scales μ_E and $\mu_m = \mu_M$ is by factor 1.5 and 1/1.5 around the values $2\pi T$ and $m_E^{(0)}(T)$ of Eq. (42), respectively. (b) Same as in Fig. (a), but now the unknown parameters δ_E and δ_G are varied, according to Eqs. (40) and (21), respectively.

However, the variation of the lower scale $\mu_m = \mu_M$ influences significantly the results for \tilde{p}_{M+G} and thus p/p_{ideal} , at $T \lesssim 1$ GeV, as seen in Figs. 11. This strong variation is a reflection of at least two aspects present at $T \lesssim 1$ GeV: (a) the scale $\mu_M = \mu_m \sim m_E^{(0)}(T)$ falls down to $\lesssim 1$ GeV, a region where the perturbative approach and RGE running eventually break down; (b) the hierarchy of scales $(2\pi T) \gg m_E^{(0)}(T)$ gets very narrowed down. The first aspect is reflected in the strong instability of the leading order QCD term $\propto g_s^3(\mu_m)$ [Eq. (32)] for the $\lambda_E^{(1)}/m_E$ -term in expansion (27) under the variation of $\mu_m (= \mu_M)$ at low T 's. This term is not included in the resummation, as emphasized earlier. The variation of this term is a major source of the appreciable variation of the p/p_{ideal} -curve at low T 's in Fig. 11(a). The variation of $\mu_M = \mu_m$ downwards to $m_E^{(0)}/1.5 = 0.73$ GeV is not allowed because the coupling parameter $g_s(\mu_m)$ blows up at such low scales by the renormalization group equation when the beta function is continued into the strong coupling region by the Padé [2/3] (as is the case in our numerical results). The renormalization scales $\mu_M = \mu_m = m_E^{(0)}/1.5$ correspond to the lower curves in Fig. 11, and they were drawn down to such temperatures where the corresponding coupling constant $a(\mu_m)$ blew up. For the other renormalization scales, the curves were drawn down to approximately such temperatures where the physically motivated condition (42) cannot be fulfilled any more.

We can apply for the $\lambda_E^{(1)}/m_E$ -term in expansion (27) of \tilde{p}_{M+G} the leading term of expansion (33) in powers of the first EQCD parameter g_E^2/m_E (with $P[1/1]$ for g_E^2 and $P[1/1]$ for m_E^2 , at renormalization scale μ_M), instead of the

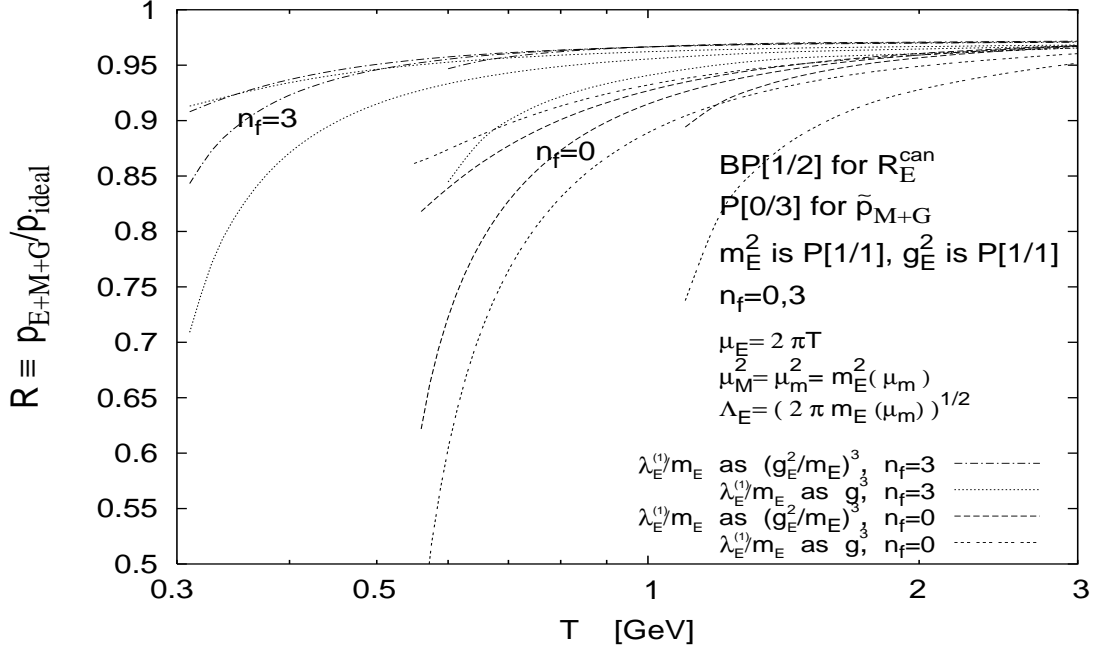


FIG. 12: Analogous to Fig. 11(a), but now the results are included when the $\lambda_E^{(1)}/m_E$ -term in expansion (27) is written as proportional to $(g_E^2/m_E)^3$ [Eq. (33)], and not g_s^3 [Eq. (32)]. The variation under the aforementioned changes of the scale $\mu_M = \mu_m$ are included; $\delta_E = \delta_G = 0$.

leading term of expansion (32) in powers of the QCD parameter $g_s(\mu_M)$. The $\lambda_E^{(1)}/m_E$ -term is again not included in the [0/3]-Padé resummation, but is added separately. These results are shown in Fig. 12, along with the results of Fig. 11. Only the variation of the curves under the aforementioned variation of the $\mu_M = \mu_m$ scales is presented. The variation of the two types of curves, at any given temperature T , under the changes of μ_E , δ_E and δ_G , is identical, thus very weak (shown in Figs. 11). We see from Fig. 12 that the variation of the curves under the changes of $\mu_M = \mu_m$ is now significantly weaker. This has primarily to do with the significantly weaker μ_M -dependence of the EQCD term $(g_E^2/m_E)^3$ of Eq. (33), in comparison to the μ_M -dependence of the the QCD term $g_s^3(\mu_M)$ of Eq. (32).

V. EVALUATIONS OF TRUNCATED PERTURBATION SERIES

Now we investigate how the results change if, instead of Padé or Borel-Padé, simple TPS evaluations are applied to all expansions: to expansion (38) for R_E^{can} , to (28) and (29) for m_E^2 and g_E^2 , and to (34) or (27) for \tilde{p}_{M+G} . The results for the pressure, as a function of temperature, for $n_f = 3$, are presented in Figs. 13(a) and 13(b), when expansions (34) and (27) are used for \tilde{p}_{M+G} , respectively. We enforce here: $\mu_M = \mu_m$; and either $\mu_m = [(m_E^2)^{(TPS)}(\mu_m)]^{1/2}$, or $\mu_m = [(m_E^2)^{P[1/1]}(\mu_m)]^{1/2}$ [the latter is $m_E^{(0)}(T)$ of Eq. (42)]. The curves with (NL)TPS m_E^2 are continued down to such temperatures where the aforementioned condition $\mu_m = m_E$ cannot be enforced any more, indicating that this (perturbative) TPS method becomes inapplicable below such temperatures $T \approx 2$ GeV. The curves with P[1/1] m_E^2 in Figs. 13 can in principle be shown, as earlier, for temperatures down to $T \approx 0.3$ GeV; however, their values (for $|\delta_E| \leq |k_2^{(0)}|$) fall drastically: $p/p_{ideal} < 0.45$ already at $T \approx 1$ GeV (which, incidentally, is far lower than the lattice results), and $p < 0$ already at $T \approx 0.5$ GeV. These curves, with P[1/1]-resummed m_E^2 and g_E^2 are presented in Figs. 14 in more detail for the low temperatures, where now $n_f = 3$ and $n_f = 0$. The $\lambda_E^{(1)}/m_E$ -term in expansion (27) is added as the term $\propto g_s^3(\mu_M)$ [Eq. (32)]. In Fig. 14(a), the variation of these TPS curves under the changes of the two renormalization scales μ_E and $\mu_M = \mu_m$, as explained for Fig. 11(a), is presented. In Fig. 14(b), the variation under the changes of the parameters δ_E and δ_G is presented. In Fig. 14(a) we see that the TPS curves vary more strongly under the changes of the high-energy scale μ_E than under those of the low-energy scale $\mu_M = \mu_m$. This result, at first sight paradoxical, occurs mainly because we used for p_{M+G} the EQCD expansion (27), with the dominant part coming from powers of the EQCD parameter g_E^2/m_E , where the μ_m -dependence of this parameter is rather weak because we used P[1/1]($a(\mu_m)$) for g_E^2 and for m_E^2 . Comparing with the corresponding Padé–Borel–Padé

(P+BP) resummed curves of Figs. 11, we see that the latter have much weaker dependence on the parameters δ_E and δ_G and on the high-energy renormalization scale μ_E , while the dependence on the low energy renormalization scale $\mu_M = \mu_m$ ($\sim m_E \sim g_s T$) is reduced by P+BP resummation only by a factor of 2-3. For example, at $T = 0.7$ GeV and $n_f = 3$, this variation is about 0.18 and 0.06 GeV in the TPS and P+BP cases, respectively. This has largely to do with the $\lambda_E^{(1)}/m_E$ -term which is not resummed in the P+BP case, but is also taken as $\propto g_s^3(\mu_M)$ [Eq. (32)] and added separately. On the other hand, taking that term as $\propto (g_E^2/m_E)^3$ [Eq. (33)], and adding it after the resummation, significantly weakened the μ_M -dependence at low temperatures, as was seen in Fig. 12.

On all these grounds, the Padé and Borel-Padé results of Figs. 11 and 12 are likely to give more realistic results at low $T \sim 1$ GeV than the corresponding TPS results.

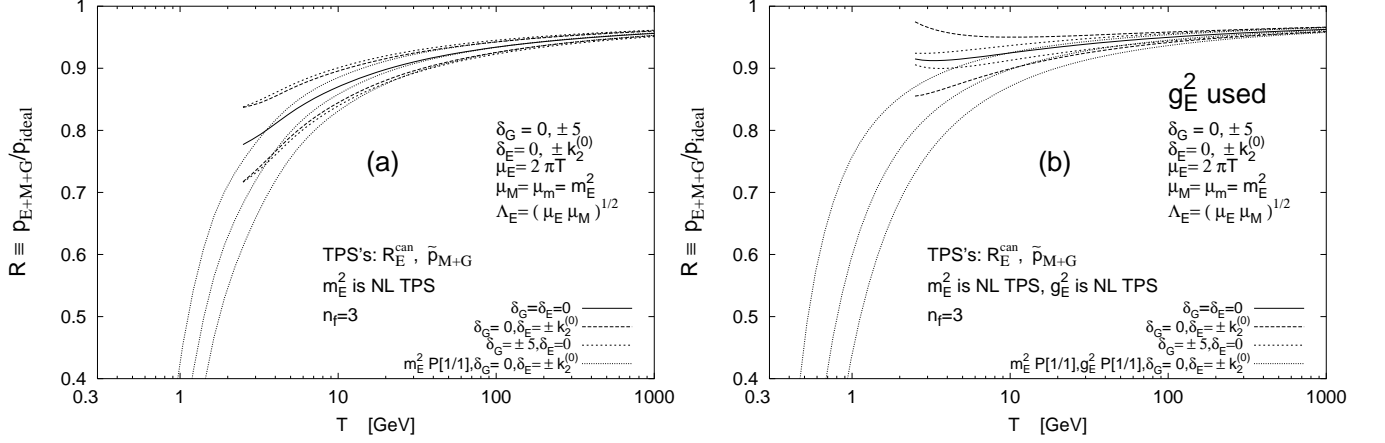


FIG. 13: (a) The total pressure as a function of temperature T when TPS evaluation is employed for R_E^{can} and \tilde{p}_{M+G} , instead of the Padé and Borel-Padé of Fig. 7; (b) Same as in (a), but now \tilde{p}_{M+G} is evaluated as expansion (27) in g_E^2/m_E . Further explanations are given in the text.

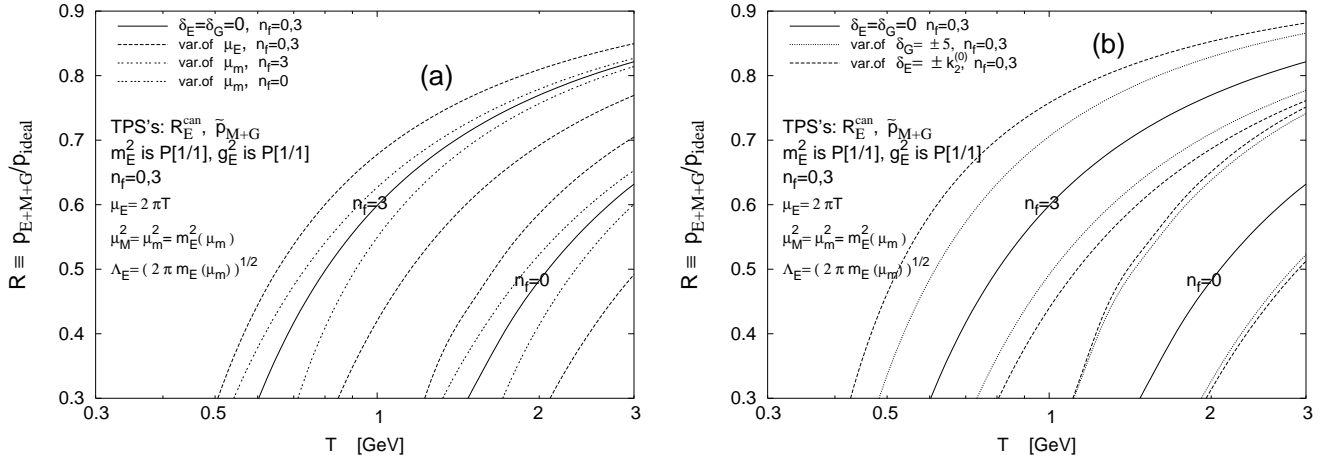


FIG. 14: (a) The low-temperature total pressure (for $n_f = 3, 0$) when TPS evaluation is employed for R_E^{can} and \tilde{p}_{M+G} , but for m_E^2 and g_E^2 Padé P[1/1]. The variation of the renormalization scales μ_E and $\mu_m = \mu_M$ is by factor 1.5 and 1/1.5 around the values $2\pi T$ and $m_E^{(0)}(T)$ of Eq. (42), respectively. (b) Same as in Fig. (a), but now the unknown parameters δ_E and δ_G are varied, according to Eqs. (40) and (21), respectively.

VI. COMPARISONS WITH OTHER APPROACHES, AND CONCLUSIONS

An approach different from our resummation is to set all ($\overline{\text{MS}}$) renormalization scales equal: $\overline{\mu} = \mu_E = \mu_m = \mu_M = \Lambda_E$, and then evaluate m_E , p_E and \tilde{p}_{M+G} ($\Rightarrow p_{M+G}$). This was the approach of Ref. [42], and the evaluation in

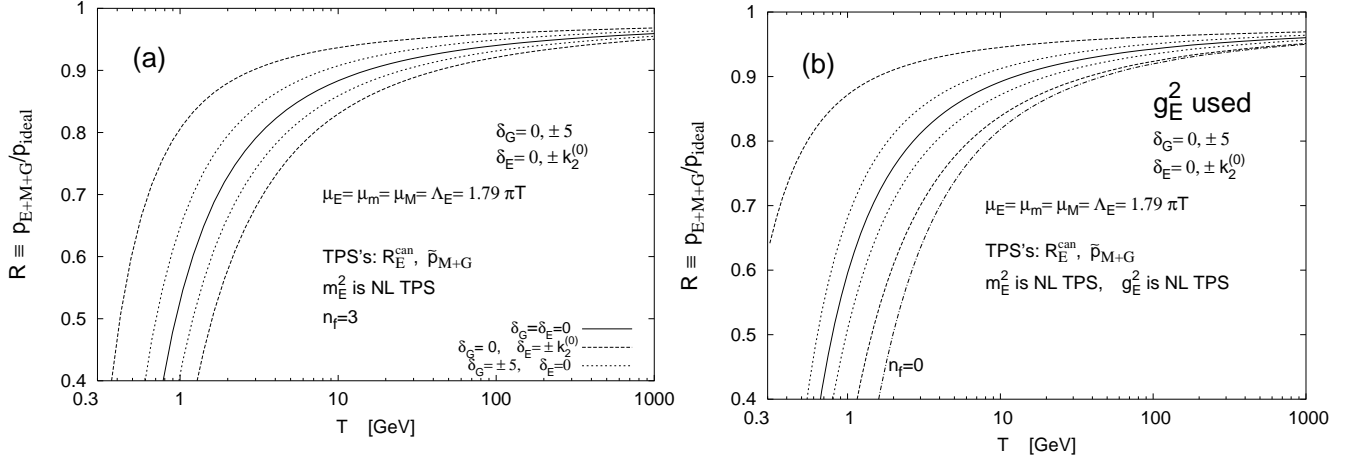


FIG. 15: (a) The total pressure (with $n_f = 3$) as a function of the temperature T when TPS evaluation is employed for R_E^{can} , m_E^2 , and \tilde{p}_{M+G} of (34), but with common scales used: $\mu_E = \mu_m = \mu_M = \Lambda_E = 1.79\pi T$. The unknown parameters δ_G and δ_E are varied in the interval (21) and (40), respectively, for $n_f = 3$. (b) same as Fig. (a), but using for p_{M+G} expansion (27) in powers of g_E^2/m_E . Further explanations are given in the text.

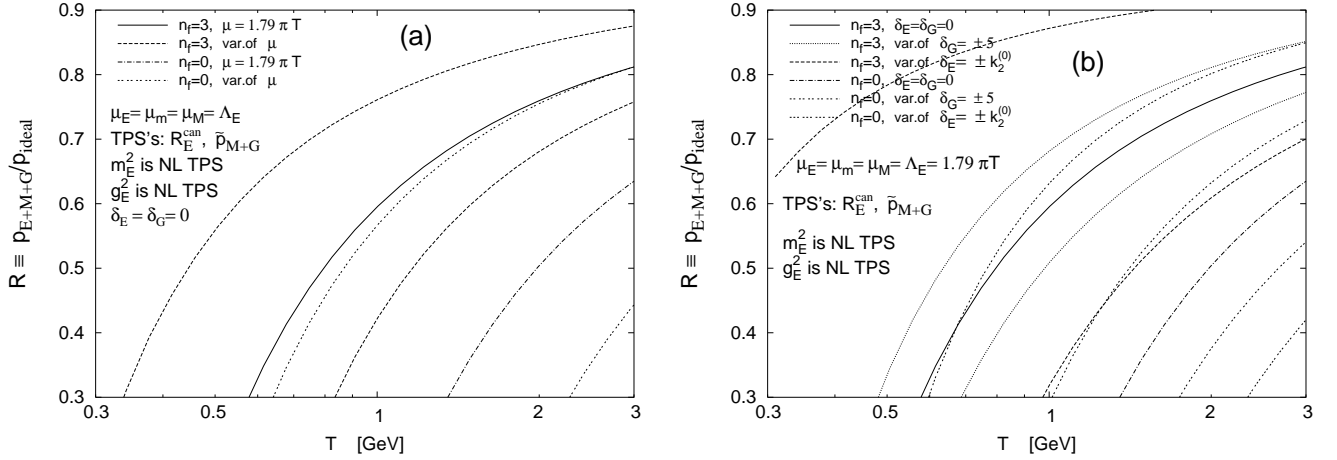


FIG. 16: (a) The low-temperature total pressure (for $n_f = 3, 0$) when TPS evaluation is employed for R_E^{can} , m_E^2 , g_E^2 , and \tilde{p}_{M+G} of Eq. (27), but with common scales used: $\mu_E = \mu_m = \mu_M = \Lambda_E = 1.79\pi T$. Variation of the scale is by factor 1.5: $\mu_{\text{max}} = 1.51.79\pi T$, $\mu_{\text{min}} = (1/1.5)1.79\pi T$. (b) The unknown parameters δ_G and δ_E are varied in the interval (21) and (40), respectively, for $n_f = 3, 0$.

Ref. [4] was similar as well. In both of these references, truncated perturbation series (TPS) evaluations were applied. In Figs. 15(a) and 15(b), we present the results of such type of resummation as a function of temperature, for $n_f = 3$, when \tilde{p}_{M+G} is evaluated as TPS (34) and TPS (27), respectively. The common scale was chosen to be $\bar{\mu} = 1.79\pi T$ and the expansions (38), (28), (29), (34) [or (27)] were evaluated as TPS. This should correspond roughly to the method leading to the the dash-dotted curve in Fig. 5 of Ref. [42] for $n_f = 0$. We can see from Figs. 15 that this approach gives, at low $T < 10$ GeV, results similar to the dotted TPS curves of Figs. 13 where $P[1/1]$ was used for m_E^2 and different renormalization scales were used for TPS p_E and TPS \tilde{p}_{M+G} . However, in contrast to Ref. [42], most of our TPS curves in Figs. 13 and 15 fall down faster than theirs when temperature decreases to $T < 1$ GeV ($T/T_c \lesssim 5$), and fall down faster than the lattice curves. Only the upper $n_f = 3$ curve in Fig. 15(b), corresponding to the choice $\delta_E = -|k_2^{(0)}|$ (and $\delta_G = 0$), is marginally compatible with the lattice results.

In Figs. 16(a) and (b) we present, at low temperatures, and for $n_f = 3$ and 0, the variation of these curves when the common renormalization scale μ changes around $1.79\pi T$ (from $1.79\pi T/1.5$ to $1.5 \times 1.79\pi T$), and when the parameters δ_E and δ_G change, respectively (in analogy with Figs. 14 and 11). We see that the variation of the curves is then similarly strong as for the TPS curves of Figs. 14.

On the other hand, Padé and Borel-Padé resummations, Figs. 8-11 (falling down as well at low decreasing T) are much less dependent on the unknown parameters δ_G and δ_E , as can be seen by comparing with the TPS curves

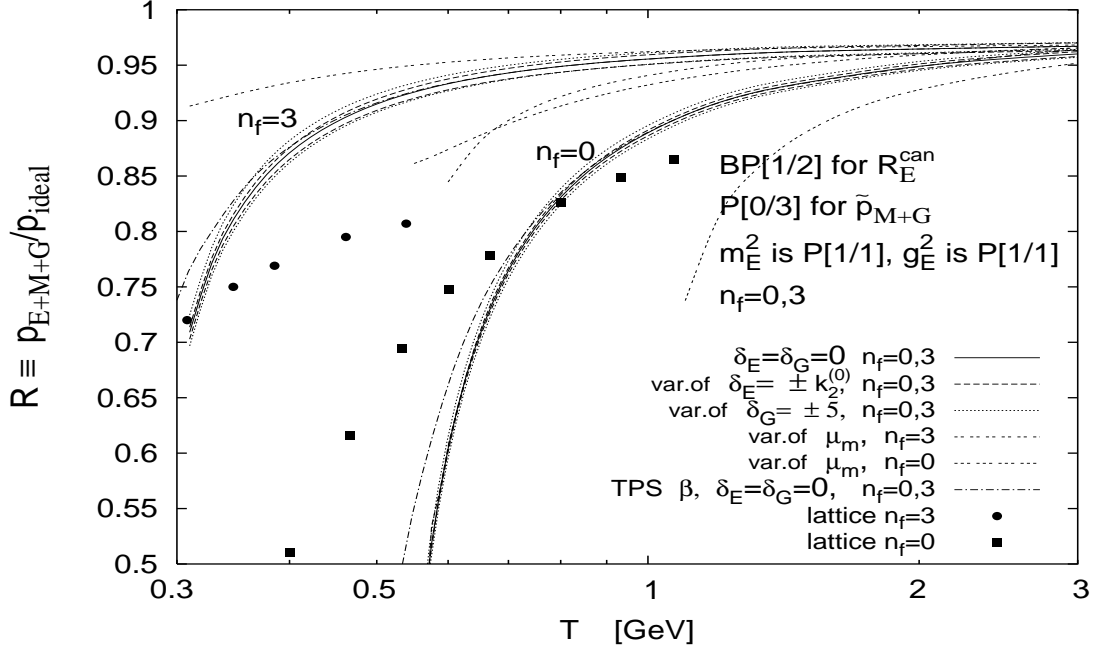


FIG. 17: Summary of our results for $n_f = 3$ and $n_f = 0$, when the unknown parameters δ_E and δ_G are varied. The resummation of ρ_{M+G} was performed on the basis of expansion (27) for $\tilde{\rho}_{M+G}$ in powers of g_E^2/m_E . Other details given in the text.

Figs. 13 and 15.

Let us now summarize our findings. We first collect the main results for the optimal approximants (which have been presented in detail in Figs. 8-12) and combine them in Figs. 17 and 18, thereby focussing on the crucial region of low temperatures. For comparison we also include the predictions of lattice calculations taken from Fig. 4(b) of Ref. [43] (which includes lattice results of Refs. [25]). These figures thus present our resummation results when Borel-Padé BP[1/2]($a(\mu_E)$) is applied to expansion (38) for R_E^{can} , and Padé [0/3](g_E^2/m_E) to expansion (27) for $\tilde{\rho}_{M+G}$. The central values of the renormalization scales were taken $\mu_E = 2\pi T$ and $\mu_M = \mu_m = m_E^{(0)}(T)$ [Eq. (42)], and the central factorization scale was $\Lambda_E = (\mu_E \mu_M)^{1/2}$. The EQCD parameters g_E^2 and m_E^2 were calculated (resummed) as Padé P[1/1]($g_s(\mu_m)$), at low-energy renormalization scale $\mu_M = \mu_m$ ($\sim m_E \sim g_s T$). In addition, the effect of replacing the Padé-resummed P[2/3](a) β function by the simple TPS β is displayed as well. For the lattice results, we used the values of critical temperature $T_c(n_f = 3) \approx 154$ MeV [43], and $T_c(n_f = 0) \approx 267$ MeV. The latter value is obtained from the result $T_c/\sqrt{\sigma} = 0.629$ [24] and $\sqrt{\sigma} = 425$ MeV [43].

The two Figures (17 and 18) differ by the different treatment of the $\lambda_E^{(1)}$ -term: In Fig. 17, the $\lambda_E^{(1)}/m_E$ -term of expansion (27) is added separately as the leading order term of expansion (32), i.e., as a term proportional to $g_s^3(\mu_m)$. In Fig. 18, on the other hand, the $\lambda_E^{(1)}/m_E$ -term is added separately as the leading order term of expansion (33), i.e., as a term proportional to $(g_E^2/m_E)^3$ [with the EQCD parameters g_E^2 and m_E^2 resummed as P[1/1]($a(\mu_m)$)]. In the latter case, the dependence on the low-energy renormalization scale $\mu_M = \mu_m$ becomes appreciably weaker, as was seen in Fig. 12 [cf. also the discussion following Eqs. (32)-(33)].

In both cases, the lattice results differ from these curves by about 20% and 10% when $n_f = 3, 0$, respectively. Taking into account that all lattice results should be taken with an error of 10-15%, we see that our resummed results come at low temperatures reasonably close to the lattice results, although our resummations are based only on perturbation expansions. Further, in contrast to the various TPS evaluations, the dependence of our results on the unknown parameters δ_G and δ_E and on the high-energy renormalization scale μ_E ($\sim 2\pi T$) is quite weak as shown in Fig. 17. The dependence on the low-energy renormalization scale $\mu_M = \mu_m$ ($\sim m_E(T)$) is in Fig. 17 by about a factor of 2-3 weaker than in the analogous TPS case, and is thus at low temperatures still quite significant. It has its origin primarily in the μ_m -dependence of the QCD term $g_s^3(\mu_m)$ of Eq. (32). In Fig. 18, the variation of the curves when δ_G , δ_E and μ_E are changed, at any given T , are identical to the variations of the corresponding curves of Fig. 17, i.e., quite weak. The dependence on the low-energy renormalization scale $\mu_m = \mu_M$ is in Fig. 18 appreciably weaker than in Fig. 17.

Let us recall also, that the specific choices for the approximants which entered in Figs. 17 and 18 were based on the following reasoning: a TPS at a given order, in principle, allows for various Padé and Borel-Padé approximants. We

chose those approximants which give results reasonably stable under the variation of the corresponding renormalization scales μ_E and $\mu_M = \mu_m$, and of the factorization scale Λ_E . This physical criterion led us to two possible approximants: BP[0/3] and P[0/3] for \tilde{p}_{M+G} ; in both cases BP[1/2] for R_E^{can} . They differed from each other significantly in the low temperature regime, cf. Fig. 9(b). In order to further eliminate one of them (BP[0/3]), we had to apply an additional physically motivated criterion, namely that the predicted pressure should be smaller than the ideal gas value if the temperature T is sufficiently near the critical value T_c . In addition, two numerical arguments were provided which also support the elimination of the approximant BP[0/3] for \tilde{p}_{M+G} . Thereby we ended up with the approximants BP[1/2] for R_E^{can} ($\Rightarrow p_E$) and P[0/3] for \tilde{p}_{M+G} ($\Rightarrow p_{M+G}$) which are considered as our “best approximants”.

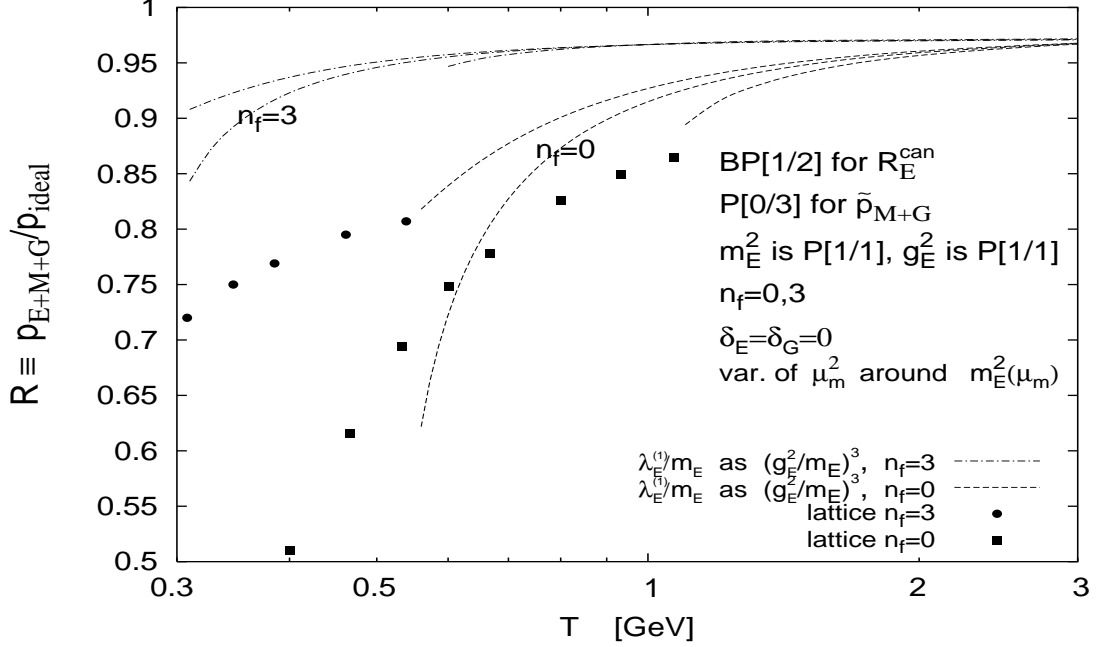


FIG. 18: Analogous to Fig. 17, but the $\lambda_E^{(1)}/m_E$ -term of Eq. (27) is now written as proportional to $(g_E^2/m_E)^3$ [Eq. (33)] instead of g_s^3 [Eq. (32)]. Changes under the variation of $\mu_M = \mu_m$ are included as in Fig. 17, and $\delta_E = \delta_G = 0$ is kept. The curves vary by the identical amounts, at any given T , as in Fig. 17 under the changes $\delta_E = \pm k_2^{(0)}$ and $\delta_G = \pm 5$.

Since both are of Padé type, we expect that they also have a better convergence behavior than the ordinary truncated perturbation theories. This, in fact, can be tested explicitly and the results are presented in Fig. 19, where we demonstrate the behavior of the Padé and Borel-Padé resummed curves, for $n_f = 3$, when the order of expansions (38) and (27) for R_E^{can} and \tilde{p}_{M+G} increases, and compare them with the corresponding TPS evaluations. For all the curves here, including the TPS curves, the EQCD parameters m_E^2 and g_E^2 were evaluated as $P[1/1](a(\mu_m))$, as in Figs. 14 and 17-18. The $\mathcal{O}(g^4)$ P-curve uses $P[1/1](a(\mu_E))$ for R_E^{can} and $P[0/1](g_E^2/m_E)$ for \tilde{p}_{M+G} of expansion (27); the $\mathcal{O}(g^5)$ P-curve uses $P[1/1]$ for R_E^{can} and $P[0/2]$ for \tilde{p}_{M+G} . The $\mathcal{O}(g^6)$ (P+BP)-curves use BP[1/2] for R_E^{can} and P[0/3] for \tilde{p}_{M+G} – the lower curve is the central curve of Fig. 17, the upper is the central curve of Fig. 18. In Fig. 19 we see that the TPS results change strongly when the order of the TPS is increased; on the contrary the resummed results suffer weaker changes, although a clear convergence at $T < 1$ GeV still cannot be seen at these orders.

The crucial point of our approach was to treat separately the short-distance (p_E) and long-distance (m_E^2, g_E^2, p_{M+G}) quantities – using in them the renormalization (and factorization) scales which correspond roughly to the physical scales of the considered quantities, and then performing either Padé or Borel-Padé resummation of each quantity. In this way we arrive at predictions for pressure which have weak dependence on the unknown parameters δ_E and δ_G , and on the high-energy renormalization scale μ_E ($\sim 2\pi T$) of p_E . On the other hand, the dependence of the predicted pressure on the renormalization scale $\mu_m = \mu_M$ ($\sim m_E$) of p_{M+G} is still large at $T \lesssim 1$ GeV when the EQCD $\lambda_E^{(1)}/m_E$ -term in the EQCD expansion (27) is added separately as a power of the QCD coupling parameter $g_s(\mu_m)$ [Eq. (32)]. This μ_m -dependence becomes significantly weaker when the EQCD $\lambda_E^{(1)}/m_E$ -term is instead added separately as a power of the first EQCD coupling parameter g_E^2/m_E [Eq. (33)]. Further, the resummed results change reasonably slowly when the order of the TPS’s, on which they are based, is increased.

On the other hand, simple TPS evaluations do not yield reasonable results for the long-distance quantities at low temperatures, because the TPS’s at such low energy scales have strong dependence on the unknown parameters and

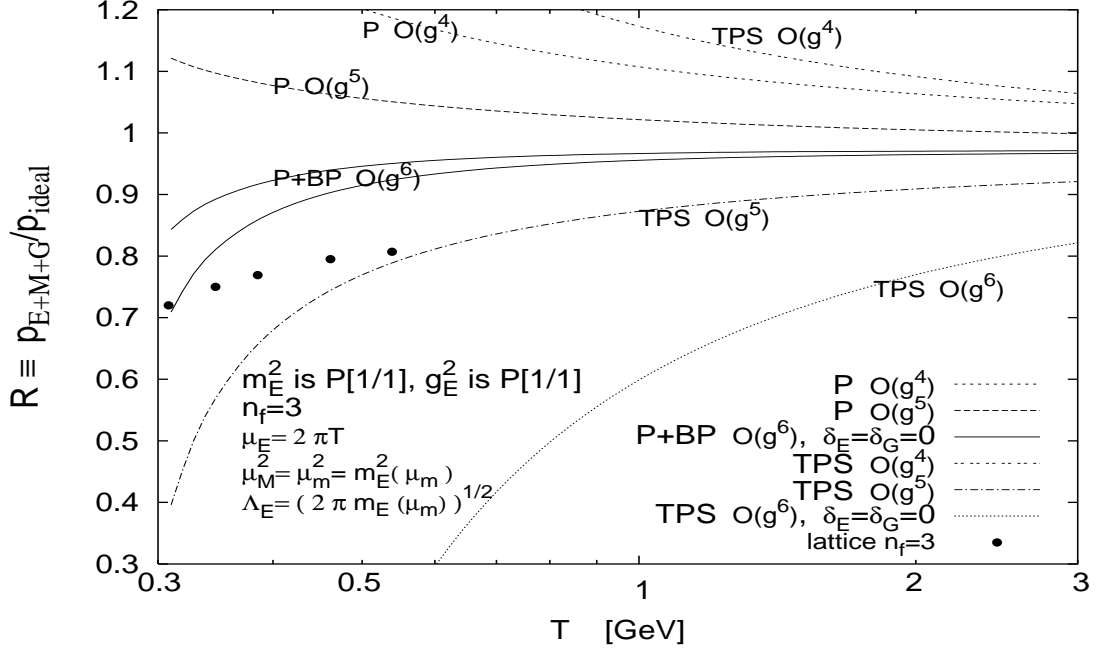


FIG. 19: The convergence behavior of our (Borel-)Padé curves for p/p_{ideal} as a function of temperature, at $n_f = 3$, for orders $\mathcal{O}(g_s^4)$, $\mathcal{O}(g_s^5)$ and $\mathcal{O}(g_s^6)$, and the behavior of the corresponding TPS's. The upper P+BP $\mathcal{O}(g_s^6)$ curve is for the case when the $\lambda_E^{(1)}/m_E$ -term of Eq. (27) is now written as proportional to $(g_E^2/m_E)^3$ instead of g_s^3 . Details are given in the text.

on the renormalization scales, and change strongly when the order of the TPS's is increased.

Acknowledgments

We thank E. Laermann, M. Laine, and H. Satz for helpful communication. This work was supported in part by FONDECYT (Chile) grant No. 1010094 (G.C.)

APPENDIX A: PADÉ AND BOREL-PADÉ APPROXIMANTS

In this Appendix, we describe the procedure we used to obtain the Padé and Borel-Padé approximants on the bases of perturbation expansions (28), (29), (34), (27) and (38). In expansions (28), (29) and (38), the expansion parameter was $a(\bar{\mu}) = [g_s(\bar{\mu})/2\pi]^2$. The canonical expansions of this type have the form:

$$S(a) = a \left(1 + \sum_{n=1}^{\infty} r_n a^n \right). \quad (\text{A1})$$

Padé approximant of order (N, M) is $P[N/M]_S(a) = P_N(a)/P_M(a)$, i.e., the ratio of polynomials $P_N(a)$ and $P_M(a)$ of order N and M , respectively. The coefficients of these polynomials are determined by the requirement that the re-expansion of the approximant in powers of a reproduce the terms up to (and including) $\sim a^{N+M}$ in the expansion (A1). For example,

$$P[1/1](a) = \frac{a}{(1 - r_1 a)}. \quad (\text{A2})$$

The Borel-Padé approximation $BP[N/M]_S(a)$ is constructed from expansion (A1) by applying Padé $P[N/M]_{B_S}(b)$ to the expansion of the Borel-transform

$$B_S(b) = 1 + \sum_{n=1}^{\infty} \frac{r_n}{n! \beta_0^n} b^n, \quad (\text{A3})$$

and then performing the Borel integration

$$\text{BP}[N/M]_S(a) = \frac{1}{\beta_0} \int_0^\infty db \exp\left(-\frac{b}{\beta_0 a}\right) \text{P}[N/M]_{B_S}(b). \quad (\text{A4})$$

In principle, the integration here is along the positive b -axis. In order to avoid any possible poles on the positive b -axis, the integration is in general performed along a ray in the b plane, say: $b = r \exp(-i\phi)$, with $\phi \neq 0$ arbitrary and fixed; then $r = |b|$ is integrated from zero to infinity, and the real part of the result is taken – cf. Ref. [37]. This leads, by Cauchy theorem, to the Principal Value (PV) prescription for integral (A4).

On the other hand, expansions (34) and (27) for \tilde{p}_{M+G} have the following form:

$$T(g) = 1 + \sum_{n=1}^{\infty} t_n g^n, \quad (\text{A5})$$

where $g \equiv g_s(\mu_M)$ or $g \equiv g_E^2/m_E$. Padé approximant $\text{P}[N/M]_T(g) = P_N(g)/P_M(g)$ was in this case simply the Padé applied to expansion (A5). The Borel-Padé approximation $\text{BP}[N/M]_T(g)$ was constructed from expansion (A5) by applying Padé $\text{P}[N/M]_{\tilde{B}_T}(z)$ to the (expansion) of the following Borel transform of T :

$$\tilde{B}_T(z) = 1 + \sum_{n=1}^{\infty} \frac{t_n}{n!} z^n, \quad (\text{A6})$$

and then performing the corresponding Borel integration

$$\text{BP}[N/M]_T(g) = \frac{1}{g} \int_0^\infty dz \exp\left(-\frac{z}{g}\right) \text{P}[N/M]_{\tilde{B}_T}(z). \quad (\text{A7})$$

Again, in order to avoid the possible poles at $z > 0$, the integration is performed along a ray in the z -plane and the real part is taken.

-
- [1] For excellent recent reviews see: U. Kraemmer and A. Rebhan, Rept. Prog. Phys. **67**, 351 (2004) [hep-ph/0310337]; J. O. Andersen and M. Strickland, hep-ph/0404164.
- [2] P. Arnold and C. x. Zhai, “The Three Loop Free Energy For Pure Gauge QCD,” Phys. Rev. D **50**, 7603 (1994) [hep-ph/9408276]; *ibid.* **51**, 1906 (1995) [hep-ph/9410360]; C. x. Zhai and B. Kastening, Phys. Rev. D **52**, 7232 (1995) [hep-ph/9507380].
- [3] E. Braaten and A. Nieto, Phys. Rev. Lett. **76**, 1417 (1996) [hep-ph/9508406]; Phys. Rev. D **53**, 3421 (1996) [hep-ph/9510408].
- [4] K. Kajantie, M. Laine, K. Rummukainen and Y. Schröder, Phys. Rev. D **67**, 105008 (2003) [hep-ph/0211321].
- [5] K. Kajantie, M. Laine, K. Rummukainen and Y. Schröder, JHEP **0304**, 036 (2003) [hep-ph/0304048].
- [6] T. S. Biró, P. Lévai and B. Müller, Phys. Rev. D **42**, 3078 (1990); A. Peshier, B. Kämpfer, O. P. Pavlenko and G. Soff, Phys. Rev. D **54**, 2399 (1996); P. Lévai and U. W. Heinz, Phys. Rev. C **57**, 1879 (1998) [hep-ph/9710463].
- [7] J. P. Blaizot, E. Iancu and A. Rebhan, Phys. Lett. B **470**, 181 (1999) [hep-ph/9910309]; Phys. Rev. Lett. **83**, 2906 (1999) [hep-ph/9906340]; Phys. Rev. D **63**, 065003 (2001) [hep-ph/0005003]; A. Peshier, Phys. Rev. D **63**, 105004 (2001) [hep-ph/0011250].
- [8] F. Karsch, A. Patkós and P. Petreczky, Phys. Lett. B **401**, 69 (1997) [hep-ph/9702376]; J. O. Andersen and M. Strickland, Phys. Rev. D **64**, 105012 (2001) [hep-ph/0105214].
- [9] S. Chiku and T. Hatsuda, Phys. Rev. D **58**, 076001 (1998) [hep-ph/9803226].
- [10] J. O. Andersen, E. Braaten and M. Strickland, Phys. Rev. Lett. **83**, 2139 (1999) [hep-ph/9902327]; Phys. Rev. D **61**, 014017 (2000) [hep-ph/9905337]; Phys. Rev. D **61**, 074016 (2000) [hep-ph/9908323]. J. O. Andersen, E. Petitgirard and M. Strickland, hep-ph/0302069.
- [11] George A. Baker, Jr. and Peter Graves-Morris, *Padé Approximants*, 2nd edition, (Encyclopedia of Mathematics and Its Applications, Vol. 59), edited by Gian-Carlo Rota (Cambridge University Press, 1996).
- [12] E. Gardi, Phys. Rev. D **56**, 68 (1997) [hep-ph/9611453].
- [13] S. J. Brodsky, J. R. Ellis, E. Gardi, M. Karliner and M. A. Samuel, Phys. Rev. D **56**, 6980 (1997) [hep-ph/9706467].
- [14] J. R. Ellis, E. Gardi, M. Karliner and M. A. Samuel, Phys. Rev. D **54**, 6986 (1996) [hep-ph/9607404]; Phys. Lett. B **366**, 268 (1996) [hep-ph/9509312]; E. Gardi, Acta Phys. Polon. B **28**, 3067 (1997) [hep-ph/9709272].
- [15] V. L. Eletsky and V. S. Popov, Phys. Lett. B **77**, 411 (1978); P. A. Rączka, Phys. Rev. D **43**, 9 (1991). U. D. Jentschura, Phys. Rev. D **62**, 076001 (2000) [hep-ph/0001135]; Phys. Rev. A **64**, 013403 (2001) [physics/0010038]; G. Cvetic and J. Y. Yu, Int. J. Mod. Phys. A **16**, 57 (2001) [hep-ph/9911376]; Mod. Phys. Lett. A **15**, 1227 (2000) [hep-ph/0003241]; D. J. Broadhurst and D. Kreimer, Phys. Lett. B **475**, 63 (2000) [hep-th/9912093].

- [16] G. Cvetic, Nucl. Phys. B **517**, 506 (1998) [hep-ph/9711406]; Phys. Rev. D **57**, 3209 (1998) [hep-ph/9711487]; Nucl. Phys. Proc. Suppl. **74**, 333 (1999) [hep-ph/9808273]; G. Cvetic and R. Kögerler, Nucl. Phys. B **522**, 396 (1998) [hep-ph/9802248].
- [17] G. Cvetic, Phys. Lett. B **486**, 100 (2000) [hep-ph/0003123]; G. Cvetic and R. Kögerler, Phys. Rev. D **63**, 056013 (2001) [hep-ph/0006098].
- [18] M. Döring and R. Kögerler, to be published.
- [19] M. Neubert, Phys. Rev. D **51**, 5924 (1995) [hep-ph/9412265].
- [20] B. Kastening, Phys. Rev. D **56**, 8107 (1997) [hep-ph/9708219]; T. Hatsuda, Phys. Rev. D **56**, 8111 (1997) [hep-ph/9708257].
- [21] G. Cvetic and R. Kögerler, Phys. Rev. D **66**, 105009 (2002) [hep-ph/0207291].
- [22] R. R. Parwani, Phys. Rev. D **63**, 054014 (2001) [hep-ph/0010234]; *ibid.* **64**, 025002 (2001) [hep-ph/0010294].
- [23] M. Loewe and C. Valenzuela, Mod. Phys. Lett. A **15**, 1181 (2000) [hep-th/9911151].
- [24] G. Boyd, J. Engels, F. Karsch, E. Laermann, C. Legeland, M. Lütgemeier and B. Petersson, Phys. Rev. Lett. **75**, 4169 (1995); [hep-lat/9506025]. Nucl. Phys. B **469**, 419 (1996) [hep-lat/9602007].
- [25] F. Karsch, E. Laermann and A. Peikert, Phys. Lett. B **478**, 447 (2000) [hep-lat/0002003].
- [26] A. Papa, Nucl. Phys. B **478**, 335 (1996) [hep-lat/9605004]; B. Beinlich, F. Karsch, E. Laermann and A. Peikert, Eur. Phys. J. C **6**, 133 (1999) [hep-lat/9707023].
- [27] E. Braaten and A. Nieto, Phys. Rev. D **51**, 6990 (1995) [hep-ph/9501375].
- [28] P. H. Ginsparg, Nucl. Phys. B **170**, 388 (1980); T. Appelquist and R. D. Pisarski, Phys. Rev. D **23**, 2305 (1981).
- [29] K. Kajantie, M. Laine, K. Rummukainen and M. E. Shaposhnikov, Nucl. Phys. B **458**, 90 (1996) [hep-ph/9508379].
- [30] D. J. Gross, R. D. Pisarski and L. G. Yaffe, Rev. Mod. Phys. **53**, 43 (1981).
- [31] A. D. Linde, Rept. Prog. Phys. **42**, 389 (1979); A. D. Linde, Phys. Lett. B **96**, 289 (1980).
- [32] E. Braaten, Phys. Rev. Lett. **74**, 2164 (1995) [hep-ph/9409434].
- [33] K. Farakos, K. Kajantie, K. Rummukainen and M. E. Shaposhnikov, Nucl. Phys. B **425**, 67 (1994) [hep-ph/9404201].
- [34] S. Nadkarni, Phys. Rev. D **38**, 3287 (1988).
- [35] N. P. Landsman, Nucl. Phys. B **322**, 498 (1989).
- [36] B. V. Geshkenbein, B. L. Ioffe and K. N. Zyablyuk, Phys. Rev. D **64**, 093009 (2001) [hep-ph/0104048].
- [37] G. Cvetic and T. Lee, Phys. Rev. D **64**, 014030 (2001) [hep-ph/0101297]; G. Cvetic, C. Dib, T. Lee and I. Schmidt, Phys. Rev. D **64**, 093016 (2001) [hep-ph/0106024].
- [38] G. Grunberg, Phys. Lett. **95B**, 70 (1980), **110B**, 501(E) (1982); **114B**, 271 (1982); Phys. Rev. D **29**, 2315 (1984).
- [39] A. L. Kataev, N. V. Krasnikov, and A. A. Pivovarov, Nucl. Phys. **B198**, 508 (1982).
- [40] A. Dhar and V. Gupta, Phys. Rev. D **29**, 2822 (1984); V. Gupta, D. V. Shirkov, and O. V. Tarasov, Int. J. Mod. Phys. A **6**, 3381 (1991).
- [41] H. Satz, Rept. Prog. Phys. **63**, 1511 (2000) [hep-ph/0007069].
- [42] J. P. Blaizot, E. Iancu and A. Rebhan, Phys. Rev. D **68**, 025011 (2003) [hep-ph/0303045].
- [43] F. Karsch, Nucl. Phys. A **698**, 199 (2002) [hep-ph/0103314], and references therein.